



HAL
open science

Alternative PDGFD rearrangements in dermatofibrosarcomas protuberans without PDGFB fusions

Béregère Dadone-Montaudié, Laurent Alberti, Adeline Duc, Lucile Delespaul, Tom Lesluyes, Gaëlle Pérot, Agnès Lançon, Sandrine Paindavoine, Ilaria Di Mauro, Jean-Yves Blay, et al.

► **To cite this version:**

Béregère Dadone-Montaudié, Laurent Alberti, Adeline Duc, Lucile Delespaul, Tom Lesluyes, et al.. Alternative PDGFD rearrangements in dermatofibrosarcomas protuberans without PDGFB fusions. *Modern Pathology*, 2018, 31 (11), pp.1683-1693. 10.1038/s41379-018-0089-4 . inserm-02440547

HAL Id: inserm-02440547

<https://inserm.hal.science/inserm-02440547>

Submitted on 15 Jan 2020

HAL is a multi-disciplinary open access archive for the deposit and dissemination of scientific research documents, whether they are published or not. The documents may come from teaching and research institutions in France or abroad, or from public or private research centers.

L'archive ouverte pluridisciplinaire **HAL**, est destinée au dépôt et à la diffusion de documents scientifiques de niveau recherche, publiés ou non, émanant des établissements d'enseignement et de recherche français ou étrangers, des laboratoires publics ou privés.

Alternative *PDGFD* rearrangements in dermatofibrosarcomas protuberans without *PDGFB* fusions

Bérengrère Dadone-Montaudié ^{1*}, Laurent Alberti ^{2,3*}, Adeline Duc ³, Lucile Delespaul ^{4,5#}, Tom Lesluyes ^{4,5#}, Gaëlle Perot ⁶, Agnes Lancon ³, Sandrine Paindavoine ³, Ilaria Di Mauro ¹, Jean Yves Blay ^{2,7}, Arnaud de la Fouchardière ³, Frédéric Chibon ^{4,6#}, Marie Karanian ³, Gaëtan MacGrogan ⁶, Valérie Kubiniek ¹, **Frédérique Keslair ¹**, Nathalie Cardot-Leccia ⁸, Audrey Michot ⁹, **Virginie Perrin ¹⁰**, **Yanis Zekri ¹⁰**, Jean-Michel Coindre ^{5,6}, Franck Tirode ^{2,10}, Florence Pedeutour ¹, Dominique Ranchere-Vince ³, François Le Loarer ^{5,6§}, Daniel Pissaloux ^{2,3§}

Authors affiliations

1 Laboratory of Solid Tumors Genetics, Institute for Research on Cancer and Aging of Nice (IRCAN) CNRS UMR 7284/INSERM U1081, Université Côte d'Azur, Centre Hospitalier Universitaire de Nice, Nice, France

2 Univ Lyon, Université Claude Bernard Lyon 1, CNRS 5286, INSERM U1052, Cancer Research Center of Lyon, France

3 Department of Biopathology, Centre Léon Bérard, Lyon, France

4 INSERM U1218 ACTION, Bordeaux, France

5 University of Bordeaux, Bordeaux, France

6 Department of Pathology, Institut Bergonié, Bordeaux, France

7 Department of Oncology, Centre Léon Bérard, Lyon, France

8 Central Laboratory of Pathology, Centre Hospitalier Universitaire de Nice, Nice, France

9 Department of Surgery, Institut Bergonié, Bordeaux, France

10 Department of Translational Research and Innovation, Centre Léon Bérard, Lyon, France

* co-performed the research

current affiliation: INSERM U1037, Cancer Research Center of Toulouse (CRCT), Institut
Claudius Regaud, IUCT-Oncopole, Toulouse, France

§ co-directed the research

Corresponding author

Daniel Pissaloux

Centre Léon Bérard, Department of Pathology, Cheney B, 28 rue Laennec, 69373 Lyon,
France

daniel.pissaloux@lyon.unicancer.fr

Running title

PDGFD rearrangements in dermatofibrosarcoma protuberans

ABSTRACT

Dermatofibrosarcoma protuberans is underlined by recurrent *COL1A1-PDGFB* fusions but approximately 4% of typical **dermatofibrosarcoma protuberans** remain negative for this translocation in routine molecular screening.

We investigated a series of 21 cases not associated with the pathognomonic *COL1A1-PDGFB* fusion on routine fluorescence in situ hybridization (FISH) testing. All cases displayed morphological and clinical features consistent with the diagnosis of **dermatofibrosarcoma protuberans**. RNA-sequencing analysis was successful in 20 cases. The classical *COL1A1-PDGFB* fusion was present in 40% of cases (n=8/20), and subsequently confirmed with a *COL1A1* break-apart FISH probe in all but one case (n=7/8). 55% of cases (n=11/20) displayed novel *PDGFD* rearrangements; *PDGFD* being fused either to the 5' part of *COL6A3* (2q37.3) (n=9/11) or *EMILIN2* (18p11) (n=2/11). All rearrangements led to in-frame fusion transcripts and were confirmed at genomic level by FISH and/or array comparative genomic hybridization. *PDGFD*-rearranged **dermatofibrosarcoma protuberans** presented clinical outcomes similar to typical **dermatofibrosarcoma protuberans**. Notably, the two *EMILIN2-PDGFD* cases displayed fibrosarcomatous transformation and homozygous deletions of *CDKN2A* at genomic level.

We report the first recurrent molecular variant of **dermatofibrosarcoma protuberans** involving *PDGFD*, which functionally mimic *bona fide* *COL1A1-PDGFB* fusions, leading presumably to a similar autocrine loop stimulating PDGFRB. This study also emphasizes that *COL1A1-PDGFB* fusions can be cytogenetically cryptic on FISH testing in a subset of cases, thereby representing a diagnostic pitfall that **pathologists** should be aware of.

Keywords

Dermatofibrosarcoma protuberans; DFSP; *PDGFD*; *COL6A3*; *EMILIN2*; gene fusion; sarcoma.

INTRODUCTION

Dermatofibrosarcoma protuberans is a superficial and locally invasive mesenchymal tumor which undergoes fibrosarcomatous transformation portending a metastatic potential in 10% of cases (1). Giant cell fibroblastoma represents a morphological variant of dermatofibrosarcoma protuberans occurring in children. Both dermatofibrosarcoma protuberans and giant cell fibroblastoma are molecularly defined by the presence of translocation (17;22)(q21.3;q13.1), which fuses *collagen type I alpha 1 chain (COL1A1)* with *platelet-derived growth factor B chain (PDGFB)* (2). Most dermatofibrosarcomas protuberans display typical morphological features including a dense storiform proliferation of cells expressing diffusely and strongly CD34 (1). Fibrous morphological variants of dermatofibrosarcoma protuberans may be confused with benign cellular fibrous histiocytomas or dermatofibromas (1). A diagnosis of dermatofibrosarcoma protuberans warrants complete surgical excision that may require large resection due to the propensity of dermatofibrosarcoma protuberans to infiltrate adjacent tissues (3). Imatinib and pazopanib therapies, which target PDGF downstream signaling, may be used in unresectable or metastatic cases (3,4). Molecular confirmation of dermatofibrosarcoma protuberans is therefore strongly recommended. *COL1A1-PDGFB* fusion gene is mostly screened with dual fusion or break-apart fluorescence *in situ* hybridization (FISH) in routine practice (5). Reverse transcription polymerase chain reaction (RT-PCR) assays are slightly less sensitive than FISH due to the variability of *COL1A1* breakpoints and require non-degraded RNA, although some studies report comparable sensitivity (6,7). Cytogenetic studies have shown that t(17;22) is mostly unbalanced, associated with supernumerary ring chromosomes, and may therefore be evidenced by array comparative genomic hybridization (8,9). Altogether, routine molecular screening remains negative in approximately 4% of otherwise typical dermatofibrosarcomas protuberans, raising clinical uncertainties and leading to render a diagnosis of dermatofibrosarcoma protuberans

lacking the canonical translocation and therefore “molecularly unconfirmed” (5). Single reports of molecular variants of dermatofibrosarcoma protuberans have been reported but no systematic study has been performed so far (10-13).

In order to identify novel fusion genes in dermatofibrosarcoma protuberans, we investigated by RNA-sequencing and array comparative genomic hybridization a series of 21 morphologically typical dermatofibrosarcomas protuberans, negative for *COL1A1-PDGFB* fusion on routine molecular testing.

MATERIALS AND METHODS

Sample selection

We identified 25 cases in our records diagnosed as dermatofibrosarcoma protuberans between 2006 and 2017 but negative on molecular testing. Cases were retrieved from the archives of the department of Genetics of University Hospital of Nice (Nice, France), and departments of Pathology of Centre Léon Bérard (Lyon, France) and Institut Bergonié (Bordeaux, France). Notably, all three participating institutions used FISH for molecular testing, but they applied two different screening strategies. First, *COL1A1-PDGFB* fusion probe followed by *PDGFB* break-apart probe in case of negative or equivocal result. Second, a screening with *PDGFB* break-apart probe in the first place, followed if negative or ambiguous by a screening with a *COL1A1* break-apart probe. Due to the evolution of molecular testing strategies over time, 7 cases of our series had not been previously tested with a *PDGFB* break apart probe. Hence, FISH analysis was completed in these cases, rendering positive results in 4 cases, which were therefore removed from the final cohort (n=21).

All cases from the series were registered in the RREPS sarcoma database, a national clinical database approved by the Commission Nationale Informatique et Libertés (CNIL) and the Comité national d'éthique.

The material used in this publication was provided by the SarcomaBCB, the Conticanet database (<https://auth.sarcomabcb.org>).

Clinical review

Clinical follow-up was obtained from the medical records of patients either available at our institutions or through corresponding clinicians. Follow-up duration was calculated from the date of the clinical detection of the lesion. Clinical data are provided in **Supplementary Table 1**.

Histopathological analyses

All cases of the final series were reviewed blindly by soft tissue expert pathologists (FLL, JMC, DRV). Fibrosarcomatous transformation was defined by the presence of a fascicular component with increased mitotic activity contrasting with the storiform pattern of the DFSP component (1). All samples were studied with a panel of antibodies available in routine including AE1/E3, CD34, S100 protein, EMA, and Ki67. Pathological data are summarized in **Supplementary Table 1**.

Fluorescence in situ hybridization (FISH) analyses

FISH analyses were performed on formalin-fixed paraffin-embedded tissue sections using commercial and custom bacterial artificial chromosome (BAC) probes. Commercial FISH probes used in the study included dual fusion probe *COL1A1/PDGFB* (#Z-2116-200, Zytovision, Bremerhaven, Germany), *PDGFB* Break Apart probe (#Z-2119-200, Zytovision), and *COL1A1* Break Apart Probe (#Z-2121-200, ZytoVision). *PDGFD*, *EMILIN2* and *COL6A3* break-apart probes were prepared with BAC listed in **Supplementary Table 2**. FISH analysis was performed by assessing at least 100 non-overlapping intact nuclei by two independent operators. The positive threshold to call the FISH assay positive was 15%. BACs were cultured and labelled as previously described (14).

Array Comparative Genomic Hybridization analyses

Genomic DNA was extracted from formalin-fixed paraffin-embedded tissue using QIAamp, DNA micro kit (Qiagen, Hilden, Germany). Genomic DNA and human reference DNA (Promega) were labeled with cyanin 5 (Cy5) and cyanine 3 (Cy3), respectively, using the Genomic DNA High-Throughput *ULS* Labeling Kit (Agilent Technologies, Santa Clara, California) and co-hybridized onto a Sureprint G3 Human CGH microarray 4x180K (Agilent) following manufacturer's recommendations. Data were analyzed by Agilent Genomic Workbench software v7.0 or by Cytogenomics software (v2.9.2.4, Agilent) and expressed according to the human reference hg19 (GRCh37, Genome Reference Consortium Human Reference 37). The identification of aberrant copy number segments was based on ADM-2 segmentation algorithm with a threshold of 6.0.

RNA-sequencing analyses

RNA sequencing was performed with formalin-fixed paraffin-embedded material in all cases. Total RNA was extracted from formalin-fixed paraffin-embedded tissue section using Trizol reagent (Thermo Fisher Scientific, Courtaboeuf, France) following manufacturers' recommendations. DNA was removed using RNase-free DNase set (Qiagen) followed by second Trizol extraction. Quantity and quality of total RNA were evaluated using NanoDrop (Thermo Fisher Scientific) and Tape Station with Hs RNA Screen Tape (Agilent) using a cut off of DV₂₀₀ (defined as the percentage of RNA fragments above 200 nucleotides) above 13%. All samples passed quality criteria. Libraries were prepared with 100 ng of total RNA using TruSeq RNA Access Library Prep Kit (Illumina, San Diego, USA). Libraries were pooled by group of 14 samples at 4 nM with 1% PhiX. Sequencing was performed (75 cycles paired end) using a NextSeq 500/550 High Output V2 kit on Illumina NextSeq 500 platform (Illumina, San Diego, CA). RNA-sequencing was successful in 20 out of 21 cases. The case with failure was ruled out from the final series as no material was available to complete its

characterization by **array comparative genomic hybridization** and FISH (final series n=20, **Table 1**).

Sequencing data (up to 15 million reads per sample) were analyzed with BaseSpace sequence Hub (Illumina). Reads were aligned with STAR and TopHat2 on GRCh 38 reference genome. The fusion transcripts were called with Manta, STAR-Fusion, FusionMap and TopHat2 fusion and validated if the Manta score was up to 0.7 and present in fusion list with TopHat2 fusion and/or STAR-Fusion and/or FusionMap (15-17).

To perform the clustering analysis, gene expression values were extracted using Kallisto v0.42.5 tool (18) with GENECODE release 23 genome annotation based on GRCh38 genome reference. Kallisto TPM expression values were transformed in $\log_2(\text{TPM}+2)$ and all samples were normalized together using the quantile method from the R limma package within R (version 3.1.1) environment. Clustering was performed with the R package Cluster v2.0.3 using Pearson correlation distance and Ward's clustering method. Significance of clusters was assessed using SigClust as previously described (19).

Reverse transcriptase-polymerase chain reaction (RT-PCR) and Sanger sequencing

In 11 cases, we performed RT-PCR to confirm either the *COL6A3-PDGFD* fusion transcript or the *EMILIN2-PDGFD* fusion transcript, using the following custom primers (designed using Primer 3 program): *COL6A3* forward primer 5'GCAAGGTCAGCTTCTAGTTCA3', *PDGFD* reverse primer 5'TGGCCAACCTTCAGCTCTTCT3' (in case number 1, 2, 4, 5, 6, 7, 8, 19), *COL6A3* forward primer 5'CAGCAAGGTCAGCTTCTAGTT3' and *PDGFD* reverse primer 5'CAGTTCCACAGCCACAATTTTC3' (in case number 3) and *EMILIN2* forward primer 5'GCCACGTCTTCCAGATTTCTA3' and *PDGFD* reverse primer 5'CAGTTCCACAGCCACAATTTTC3' (in case number 9, 10). Fusion transcripts were sequenced by Sanger after extraction and enzymatic purification of RT-PCR product using High pure PCR product purification kit (Roche Diagnostics, Meylan, France).

RESULTS

Clinicopathological features

All cases were located in classical anatomical sites including trunk (n=11/20), limbs (n=6/20) and head and neck (n=3/20) (**Table 1**). Patients' age ranged from 4 to 73 years old. Clinically, lesions presented with a classical scar-like appearance (n=2), slow-growing cutaneous plaques (n=1) or cutaneous plaques with red discoloration (n=2). Additionally, one case had a multinodular presentation. All tumors displayed outcomes in line with the local malignant potential of **dermatofibrosarcoma protuberans** with late local recurrences occurring up to 12 years after initial resection (**Supplementary Table 1**). All cases presented morphological features either typical of **dermatofibrosarcoma protuberans** (n=12/20) (**Figure 1 and 2**) or consistent with a morphological variant of **dermatofibrosarcoma protuberans** including fibrous pattern (n=5/20), pigmented pattern (also referred to as Bednar tumor) (n=1/20) or hybrid Bednar/**dermatofibrosarcoma protuberans** variant with focal presence of pigments or giant cells (n=2/20) (**Supplementary Table 1**). Four cases displayed fibrosarcomatous transformation (**Figure 3**). All but two cases showed classical honeycomb infiltrative borders. Five cases were deeply located in hypodermis without dermal infiltration.

RNA-sequencing

Classical *COL1A1-PDGFB* fusions were found in 8 cases (n=8/20). *PDGFB* breakpoint was constantly found in exon 2 while breakpoints in *COL1A1* varied from exons 11 to 45 (**Supplementary Table 3**).

PDGFD rearrangements were found in eleven cases (n=11/20), *PDGFD* being fused either to collagen type VI alpha 3 chain (*COL6A3*) at 2q37 (n=9/11) or elastin microfibril Interface 2 (*EMILIN2*) at 18p11 (n=2/11). Breakpoints in *COL6A3* involved either exon 42 (n=8/9) or

exon 43 (n=1/9), while breakpoint in *PDGFD* constantly involved exon 6 (**Figure 2**) and breakpoints in *EMILIN2* were located within exon 4 (**Figure 3**).

One case (case number 20) failed to show a fusion transcript by RNA-sequencing with the different algorithms.

FISH and RT-PCR

COL6A3-PDGFD transcript and *EMILIN2-PDGFD* transcript were confirmed by RT-PCR in all cases (case number 1-10 and 19). Regarding cases with *COL1A1-PDGFB* fusions, FISH analyses were completed with a *COL1A1* break-apart probe, which was positive in 7/8 cases (**Figure 1**). Regarding cases with *PDGFD* fusions, FISH analyses were carried out with *PDGFD* break-apart probe which was positive in 9 cases out of 11 (n=9/11). Gene partners fused to *PDGFD* were also assessed with *COL6A3* and *EMILIN2* break-apart probes (**Figure 2** and **3**, respectively), showing rearrangements in 5/7 and 2/2 cases, respectively (**Supplementary Table 3**).

Array comparative genomic hybridization

On profiles, all cases with cryptic *COL1A1-PDGFB* highlighted genomic breakpoints within *COL1A1* with a genomic gain in flanking region 17q21.33-qter (n=5/5). Additional non-recurrent copy number alterations were present in all cases. Genomic gains were seen in 1q21-q25.3, 4q28-q35, 6p, 7pter, 22q11 in one case each. Whole chromosome gains involved chromosomes 6, 7, 10 and genomic loss were seen in 1q22-23 6q12-q26 and 8p in one case each (**Supplementary Table 3**).

Array comparative genomic hybridization analysis of the dermatofibrosarcomas protuberans with *COL6A3-PDGFD* fusion highlighted no breakpoint within *PDGFB* nor *COL1A1* but within *COL6A3* and *PDGFD* in 4/7 and 6/8 cases, respectively. Copy number alterations were present in the regions flanking the breakpoints in all but one case (n=6/7). Additional non-recurrent copy number alterations included gain of chromosome 12 (n=1/7), loss of 3q

(n=1/7), gains of chromosomes 1, 7 and 17 (n=1/7). The genomic profiles of the 2 cases of *EMILIN2-PDGFD* dermatofibrosarcoma protuberans displayed breakpoints within *PDGFD* (n= 1/2), without copy number alteration involving *EMILIN2*. Interestingly, both profiles presented homozygous deletion of *CDKN2A* locus (n=2/2). None of these cases displayed copy number alterations in the genomic regions flanking the breakpoints.

Clustering analysis

To assess whether *PDGFD*-rearranged dermatofibrosarcoma protuberans were biologically similar to *PDGFB*-rearranged dermatofibrosarcoma protuberans, we compared the RNA-seq expression profiles of samples of our cohort (including 5 *PDGFB*- and 9 *PDGFD*-rearranged dermatofibrosarcoma protuberans) to other spindled cutaneous neoplasms including infantile fibrosarcomas (n=7), clear cell sarcomas of soft tissue (n=2), *ALK*-rearranged Spitzoid neoplasms (n=5), *NTRK1/3*-rearranged Spitzoid neoplasms (n=7) and conventional *PDGFB*-rearranged dermatofibrosarcomas protuberans positive for gene rearrangement upon routine molecular screening (n= 3) (**Supplementary Table 4**). All cases clustered together with transcriptional profiles distinct from *ALK*- and *NTRK1/3*-rearranged Spitzoid proliferations and infantile fibrosarcomas. The dermatofibrosarcoma protuberans cluster lumped together all dermatofibrosarcoma protuberans including those with *PDGFB* fusions (both cryptic and overt rearrangements) and *PDGFD* fusions (**Figure 4**).

DISCUSSION

Dermatofibrosarcoma protuberans has historically been defined by the presence of recurrent *COL1A1-PDGFB* fusions which lead to the upregulation of PDGFRB signaling through an autocrine activating loop (20-23). However, approximately 4% of dermatofibrosarcoma protuberans prove negative for the translocation upon routine FISH testing (5).

We evidenced by RNA-sequencing that molecularly unconfirmed **dermatofibrosarcoma protuberans** displayed “cryptic” *COL1A1-PDGFB* fusions in 40% of cases (n=8/20). All **dermatofibrosarcomas protuberans** associated with “cryptic” fusions involved previously reported *COL1A1* breakpoints which position have been shown to vary considerably from exon 7 to exon 49. Interestingly, all cases displayed visible genomic breakpoints within *COL1A1* on **quantitative genomic** profiles along with and/or gains of the 17q locus flanking the breakpoint (n=5/5) (**Figure 1**). Notably, subsequent FISH analyses with *COL1A1* break-apart probe were positive in all but one case (n=7/8). Altogether, our findings support that array **comparative genomic hybridization** or screening with *COL1A1* break-apart probe may support the diagnosis of cryptic **dermatofibrosarcoma protuberans**. This complementary screening strategy remains cost-effective as compared to the cost of RNA-sequencing performed in all cases suspicious of **dermatofibrosarcoma protuberans**. Cryptic rearrangements have also been reported in other translocation-related sarcomas and are thought to be related to structural variations of the translocation or induction of neo-exons secondary to splicing variations (24-28).

Secondly, we report herein that 55% (n=11/20) of cytogenetically negative-**dermatofibrosarcoma protuberans** are associated with alternative rearrangements involving *PDGFD*. Two different types of fusion transcripts were evidenced with the 3' part of *PDGFD* being fused to the 5' part either of *COL6A3* (n=9/11) or *EMILIN2* (n=2/11). *PDGFD*, located at 11q22.3, encodes a protein belonging to the same family of *platelet-derived growth factor* than PDGFB (29). PDGFD is able to bind to PDGF receptor B (PDGFRB) (30,31). *PDGFD* has oncogenic properties through promotion of cell proliferation and angiogenesis (29) and its overexpression has been linked to a variety of malignancies (32-35). The breakpoint was constantly located within exon 6, preserving the binding domain to PDGF receptors in a similar manner than translocations involving *PDGFB*. Interestingly, the loss of exon 6 have

been shown to induce truncation due to a premature stop codon in mice, therefore a breakpoint located downstream exon 6 might jeopardize PDGFD signaling (36). *COL6A3*, located at 2q37.3, encodes a protein of extracellular matrix involved in cellular adhesion belonging to the same superfamily as *COL1A1* (37). *COL6A3* contains 3152 amino acids-long alpha3 chains which have the same sequence as alpha1 chains and harbor the same triple-helical and von Willebrand factor A domains (37). Notably, somatic rearrangements of *COL6A3* have been previously reported in tenosynovial giant cell tumors in which *COL6A3* is fused to *Colony Stimulating Factor 1 (CSF1)* (38,39). In addition, overexpression of *COL6A3* has been described in a wide array of malignancies including gastric (40), ovarian (41), colorectal (42,43) and pancreatic cancers (44). It has also been correlated to resistance to chemotherapy (41,45). The breakpoint occurred in exon 42 of *COL6A3* in all but one case (n=8/9), in contrast to the frequent variations seen in *COL1A1*. All *COL6A3-PDGFD* cases displayed genomic imbalances in regions flanking the breakpoints of *COL6A3* and/or *PDGFD* and three cases displayed additional copy number alterations (n=3/7). The morphological and clinical features of *COL6A3*-rearranged dermatofibrosarcoma protuberans did not differ from those seen in bona fide dermatofibrosarcoma protuberans. The second fusion partner *EMILIN2* was involved in 2/11 cases a. *EMILIN2*, located at 18p11.32-p11.31, encodes a glycoprotein related to the superfamily of collagen which contains collagen-like domains (37). *EMILIN2* assembles into multimers, involved in the composition of extracellular matrix (46,47). The genomic breakpoints were located constantly in exons 4 and 6 of *EMILIN2* and *PDGFD*, respectively. The fusion preserved preserves key structural domains of *EMILIN2*, including EMI domain, coiled-coil structures and leucine zippers and gC1q domain (46,47). *EMILIN2-PDGFD* dermatofibrosarcoma protuberans displayed homozygous deletion of *CDKN2A* in both cases (n=2/2). Interestingly, both cases displayed fibrosarcomatous transformation and were deep-seated within hypodermis without dermal

connection. It is notable that homozygous deletions of *CDKN2A* are linked to malignancy in varied tumor types including mesenchymal, melanocytic and epithelial neoplasms (48-50). Therefore, this alteration may portend an increased malignant potential in this subset of dermatofibrosarcoma protuberans which warrants further studies on larger cohorts with longer follow-up to assess whether the behavior of cases of *EMILIN2-PDGFD* dermatofibrosarcoma protuberans is similar or not to classical and *COL6A3-PDGFD*-associated cases.

Altogether, *PDGFD* rearrangements may functionally mimic the biology of *COL1A1-PDGFB* fusions as it involves functionally related genes and display a similar structure. Rearrangements might therefore be targeted by imatinib as classical dermatofibrosarcoma protuberans.

In conclusion, we report herein new and recurrent molecular variants of dermatofibrosarcoma protuberans underlined by *PDGFD* rearrangements, which are clinically, morphologically and molecularly indistinguishable from *COL1A1-PDGFB* dermatofibrosarcoma protuberans. Furthermore, we showed that roughly half of cases of dermatofibrosarcoma protuberans negative upon routine FISH screening are associated with cryptic *COL1A1-PDGFB* rearrangements that may be identified by array comparative genomic hybridization or FISH with a *COL1A1* break-apart probe. The functional similarities between the classical *COL1A1-PDGFB* and the alternative *COL6A3-PDGFD* or *EMILIN2-PDGFD* transcripts suggest they activate an analogous oncogenic autocrine loop involving PDGFRB signaling.

Acknowledgements

The authors wish to thank pathologists and clinicians who provided samples and clinical follow-up: M Chargeboeuf (Lons le Saunier), C Charon-Barra (Dijon), C Delfour (Montpellier), S Depardieu (Metz), A Leroux (Vandoeuvre les Nancy), A Lipandy (Nimes), E

Maubec (Paris), C de Mauroy (Rouen), YM Robin (Lille), JF Totton (Besancon), M Battistella (Paris) and MP Wissler (Villeurbanne). The authors are grateful for their insights and participation in this study to A Bazin, AC Peyron and A Ribeiro.

This work was supported by grants from La Ligue contre le Cancer de l'Ain et de Savoie, Institut National du Cancer (NETSARC, RREPS, RESOS).

Disclosure / Conflict of Interest

The authors declare no conflict of interest.

Supplementary information is available at Modern Pathology's website.

References

- 1 Mentzel T, Pedeutour F, Lazar A and Coindre JM. Dermatofibrosarcoma protuberans. In: Fletcher CDM, Bridge JA, Hogendoorn PCW and Mertens, editors. WHO classification of tumours of soft tissue and bone. 4th ed. Lyon: IARC, 2013. p.77-79
- 2 Simon MP, Pedeutour F, Sirvent N, et al. Deregulation of the platelet-derived growth factor B-chain gene via fusion with collagen gene COL1A1 in dermatofibrosarcoma protuberans and giant-cell fibroblastoma. *Nat Genet* 1997;15:95-98
- 3 Saiag P, Grob J-J, Lebbe C, et al. Diagnosis and treatment of dermatofibrosarcoma protuberans. European consensus-based interdisciplinary guideline. *Eur J Cancer* 2015;51:2604-2608
- 4 Stacchiotti S, Pantaleo MA, Negri T, et al. Efficacy and Biological Activity of Imatinib in Metastatic Dermatofibrosarcoma Protuberans (DFSP). *Clin Cancer Res* 2016;22:837-846
- 5 Karanian M, Pérot G, Coindre J-M, et al. Fluorescence in situ hybridization analysis is a helpful test for the diagnosis of dermatofibrosarcoma protuberans. *Mod Pathol* 2015;28:230-237
- 6 Salgado R, Llombart B, M Pujol R, et al. Molecular diagnosis of dermatofibrosarcoma protuberans: a comparison between reverse transcriptase-polymerase chain reaction and fluorescence in situ hybridization methodologies. *Genes Chromosomes Cancer* 2011;50:510-517
- 7 Patel KU, Szabo SS, Hernandez VS, et al. Dermatofibrosarcoma protuberans COL1A1-PDGFB fusion is identified in virtually all dermatofibrosarcoma protuberans cases when investigated by newly developed multiplex reverse transcription polymerase chain reaction and fluorescence in situ hybridization assays. *Hum Pathol* 2008;39:184-193
- 8 Linn SC, West RB, Pollack JR, et al. Gene expression patterns and gene copy number

changes in dermatofibrosarcoma protuberans. *Am J Pathol* 2003;163:2383-2395

9 Sirvent N, Maire G, Pedeutour F. Genetics of dermatofibrosarcoma protuberans family of tumors: from ring chromosomes to tyrosine kinase inhibitor treatment. *Genes Chromosomes Cancer* 2003;37:1-19

10 Nakamura I, Kariya Y, Okada E, et al. A Novel Chromosomal Translocation Associated With COL1A2-PDGFB Gene Fusion in Dermatofibrosarcoma Protuberans: PDGF Expression as a New Diagnostic Tool. *JAMA Dermatol* 2015;151:1330-1337

11 Bianchini L, Maire G, Guillot B, et al. Complex t(5;8) involving the CSPG2 and PTK2B genes in a case of dermatofibrosarcoma protuberans without the COL1A1-PDGFB fusion. *Virchows Arch Int J Pathol* 2008;452:689-696

12 Saab J, Rosenthal IM, Wang L, et al. Dermatofibrosarcoma Protuberans-Like Tumor With COL1A1 Copy Number Gain in the Absence of t(17;22). *Am J Dermatopathol* 2017;39:304-309

13 Sinovic J, Bridge JA. Translocation (2;17) in recurrent dermatofibrosarcoma protuberans. *Cancer Genet Cytogenet.* 1994;75:156-7.

14 Sirvent N, Coindre J-M, Maire G, et al. Detection of MDM2-CDK4 amplification by fluorescence in situ hybridization in 200 paraffin-embedded tumor samples: utility in diagnosing adipocytic lesions and comparison with immunohistochemistry and real-time PCR. *Am J Surg Pathol* 2007;31:1476-1489

15 Trapnell C, Roberts A, Goff L, et al. Differential gene and transcript expression analysis of RNA-seq experiments with TopHat and Cufflinks. *Nat Protoc* 2012;7:562-578

16 Ge H, Liu K, Juan T, et al. FusionMap: detecting fusion genes from next-generation sequencing data at base-pair resolution. *Bioinforma Oxf Engl* 2011;27:1922-1928

17 Lågstad S, Zhao S, Hoff AM, et al. chimeraviz: a tool for visualizing chimeric RNA. *Bioinforma Oxf Engl* 2017;33:2954-2956

- 18** Bray NL, Pimentel H, Melsted P, et al. Near-optimal probabilistic RNA-seq quantification. *Nat Biotechnol* 2016;34:525-527
- 19** Le Loarer F, Watson S, Pierron G, et al. SMARCA4 inactivation defines a group of undifferentiated thoracic malignancies transcriptionally related to BAF-deficient sarcomas. *Nat Genet* 2015;47:1200-1205
- 20** Simon MP, Pedeutour F, Sirvent N, et al. Deregulation of the platelet-derived growth factor B-chain gene via fusion with collagen gene COL1A1 in dermatofibrosarcoma protuberans and giant-cell fibroblastoma. *Nat Genet* 1997;15:95-98
- 21** Greco A, Fusetti L, Villa R, et al. Transforming activity of the chimeric sequence formed by the fusion of collagen gene COL1A1 and the platelet derived growth factor b-chain gene in dermatofibrosarcoma protuberans. *Oncogene* 1998;17:1313-1319
- 22** Shimizu A, O'Brien KP, Sjöblom T, et al. The dermatofibrosarcoma protuberans-associated collagen type Ialpha1/platelet-derived growth factor (PDGF) B-chain fusion gene generates a transforming protein that is processed to functional PDGF-BB. *Cancer Res* 1999;59:3719-3723
- 23** Sjöblom T, Shimizu A, O'Brien KP, et al. Growth inhibition of dermatofibrosarcoma protuberans tumors by the platelet-derived growth factor receptor antagonist STI571 through induction of apoptosis. *Cancer Res* 2001;61:5778-5783
- 24** Brassesco MS, Cortez MA, Valera ET, et al. Cryptic SYT/SXX1 fusion gene in high-grade biphasic synovial sarcoma with unique complex rearrangement and extensive BCL2 overexpression. *Cancer Genet Cytogenet* 2010;196:189-193
- 25** Torres L, Lisboa S, Cerveira N, et al. Cryptic chromosome rearrangement resulting in SYT-SSX2 fusion gene in a monophasic synovial sarcoma. *Cancer Genet Cytogenet* 2008;187:45-49
- 26** Lestou VS, O'Connell JX, Robichaud M, et al. Cryptic t(X;18), ins(6;18), and SYT-

SSX2 gene fusion in a case of intraneural monophasic synovial sarcoma. *Cancer Genet Cytogenet* 2002;138:153-156

27 Kovar H, Jugovic D, Melot T, et al. Cryptic exons as a source of increased diversity of Ewing tumor-associated EWS-FLI1 chimeric products. *Genomics* 1999;60:371-374

28 Chen S, Deniz K, Sung Y-S, et al. Ewing sarcoma with ERG gene rearrangements: A molecular study focusing on the prevalence of FUS-ERG and common pitfalls in detecting EWSR1-ERG fusions by FISH. *Genes Chromosomes Cancer* 2016;55:340-349

29 Wang Z, Kong D, Li Y, et al. PDGF-D signaling: a novel target in cancer therapy. *Curr Drug Targets* 2009;10:38-41

30 Bergsten E, Uutela M, Li X, et al. PDGF-D is a specific, protease-activated ligand for the PDGF beta-receptor. *Nat Cell Biol* 2001;3:512-516

31 LaRochelle WJ, Jeffers M, McDonald WF, et al. PDGF-D, a new protease-activated growth factor. *Nat Cell Biol* 2001;3:517-521

32 Torres-Martin M, Lassaletta L, Isla A, et al. Global expression profile in low grade meningiomas and schwannomas shows upregulation of PDGFD, CDH1 and SLIT2 compared to their healthy tissue. *Oncol Rep* 2014;32:2327-2334

33 Ustach CV, Kim H-RC. Platelet-derived growth factor D is activated by urokinase plasminogen activator in prostate carcinoma cells. *Mol Cell Biol* 2005;25:6279-6288

34 Wang Z, Kong D, Banerjee S, et al. Down-regulation of platelet-derived growth factor-D inhibits cell growth and angiogenesis through inactivation of Notch-1 and nuclear factor-kappaB signaling. *Cancer Res* 2007;67:11377-11385

35 Xu L, Tong R, Cochran DM, et al. Blocking platelet-derived growth factor-D/platelet-derived growth factor receptor beta signaling inhibits human renal cell carcinoma progression in an orthotopic mouse model. *Cancer Res* 2005;65:5711-5719

36 Reigstad LJ, Varhaug JE, Lillehaug JR. Structural and functional specificities of

PDGF-C and PDGF-D, the novel members of the platelet-derived growth factors family.

FEBS J 2005;272:5723-5741

37 Ricard-Blum S. The collagen family. Cold Spring Harb Perspect Biol 2011;3:a004978

38 West RB, Rubin BP, Miller MA, et al. A landscape effect in tenosynovial giant-cell tumor from activation of CSF1 expression by a translocation in a minority of tumor cells.

Proc Natl Acad Sci U S A 2006;103:690-695

39 Möller E, Mandahl N, Mertens F, et al. Molecular identification of COL6A3-CSF1 fusion transcripts in tenosynovial giant cell tumors. Genes Chromosomes Cancer 2008;47:21-25

40 Xie X, Liu X, Zhang Q, et al. Overexpression of collagen VI $\alpha 3$ in gastric cancer.

Oncol Lett 2014;7:1537-1543

41 Sherman-Baust CA, Weeraratna AT, Rangel LBA, et al. Remodeling of the extracellular matrix through overexpression of collagen VI contributes to cisplatin resistance in ovarian cancer cells. Cancer Cell 2003;3:377-386

42 Qiao J, Fang C-Y, Chen S-X, et al. Stroma derived COL6A3 is a potential prognosis marker of colorectal carcinoma revealed by quantitative proteomics. Oncotarget

2015;6:29929-29946

43 Yu J, Wu WKK, Li X, et al. Novel recurrently mutated genes and a prognostic mutation signature in colorectal cancer. Gut 2015;64:636-645

44 Arafat H, Lazar M, Salem K, et al. Tumor-specific expression and alternative splicing of the COL6A3 gene in pancreatic cancer. Surgery 2011;150:306-315

45 Park J, Morley TS, Scherer PE. Inhibition of endotrophin, a cleavage product of collagen VI, confers cisplatin sensitivity to tumours. EMBO Mol Med 2013;5:935-948

46 Mongiat M, Mungiguerra G, Bot S, et al. Self-assembly and supramolecular organization of EMILIN. J Biol Chem 2000;275:25471-25480

- 47 Colombatti A, Spessotto P, Doliana R, et al. The EMILIN/Multimerin family. *Front Immunol* 2011;2:93
- 48 Hwang HC, Sheffield BS, Rodriguez S, et al. Utility of BAP1 Immunohistochemistry and p16 (CDKN2A) FISH in the Diagnosis of Malignant Mesothelioma in Effusion Cytology Specimens. *Am J Surg Pathol* 2016;40:120-126
- 49 Li Z, Gonzalez CL, Wang B, et al. Cdkn2a suppresses metastasis in squamous cell carcinomas induced by the gain-of-function mutant p53(R172H). *J Pathol* 2016;240:224-234
- 50 Rebouissou S, Hérault A, Letouzé E, et al. CDKN2A homozygous deletion is associated with muscle invasion in FGFR3-mutated urothelial bladder carcinoma. *J Pathol* 2012;227:315-324

Figure legends

Figure 1. Cryptic *COL1A1-PDGFB* fusion in dermatofibrosarcoma protuberans. A-B.

Band-like infiltration of hypodermis and subcutaneous adipose tissue (case number 15, HES staining, x2,5 and X6,5 magnifications, respectively) **C.** Storiform proliferation infiltrating hypodermis with a honeycomb pattern (HES, X200 magnification). **D-E.** High power field view of tumour cell nuclei displaying ovoid shape and monomorphism (**D**) and focal interspersed multinucleated cells (**E**) (HES, X200 magnification) **F.** Fluorescence *in situ* hybridization (FISH) using *COL1A1* break-apart probe. FISH analysis shows an unbalanced translocation with a gain of the 5' part of *COL1A1* (probe labelled in red). **G.** Array-comparative genomic hybridization profile harbors a genomic breakpoint at *COL1A1* locus with a 5' *COL1A1* gain but no breakpoint at *PDGFB* locus (chromosome 22 view not shown). Additional copy number alterations include gains of 4q28-q35, 6p and whole chromosome 7.

Figure 2. *COL6A3-PDGFD* dermatofibrosarcoma protuberans. A.

Biopsy specimen highlighting deep-seated dense nodular proliferation (case number 6, HES staining, X20 magnification). **B.** Storiform proliferation with honeycomb infiltrative pattern typical of dermatofibrosarcoma protuberans (HES, X200). **C.** Fibrous stromal changes focally interposed between tumor cells (HES, X250) **D.** Tumor cells display ovoid monomorphic nuclei (HES, X400). **E** Array-comparative genomic hybridization profile showing deletions and breakpoints involving *COL6A3* and *PDGFD*. Additional copy number alteration includes gain of chromosome 12. **F-G.** Fluorescence *in situ* hybridization (FISH) using *COL6A3* break-apart probe (**F**) and *PDGFD* break-apart probe (**G**) showing an unbalanced rearrangement with loss of the 3' *COL6A3* and the 5' *PDGFD*, respectively. **H.** Structure of *COL6A3-PDGFD* fusion transcript. From top to bottom: scheme representing locus and chromosomal position of *COL6A3* and *PDGFD*; schematic of breakpoints positions involving *COL6A3* exon 42 and *PDGFD* exon 6; nucleotide sequence of adjoined sequences.

Figure 3. *EMILIN2-PDGFD* dermatofibrosarcoma protuberans. **A.** Biopsy specimen highlighting densely cellular tumor infiltrating hypodermis (case number 9, HES staining, X2 magnification). **B.** Focal collagenized stroma arranged in elongated fascicles suspicious for fibrosarcomatous transformation (X200 magnification). **C.** Tumor cells display ovoid monomorphic nuclei embedded in a collagenous stroma (X400 magnification). **D.** CD34 staining in this case (X250 magnification). **E.** Array-comparative genomic hybridization profile showing a homozygous deletion of *CDKN2A* (P16) but no breakpoint within *EMILIN2* or *PDGFD* loci. **F-G.** Fluorescence *in situ* hybridization (FISH) using *EMILIN2* break-apart probe (**F**) and *PDGFD* break-apart probe (**G**) showing a rearrangement of the *EMILIN2* and *PDGFD* loci, respectively. **H.** Structure of *EMILIN2-PDGFD* fusion. From top to bottom scheme representing locus and chromosomal position of *EMILIN2* and *PDGFD*; schematic of breakpoints positions which constantly occurred in exon 4 of *EMILIN2* and in exon 6 of *PDGFD*; nucleotide sequence of adjoined sequences.

Figure 4. Transcriptomic classification of dermatofibrosarcoma protuberans.

Unsupervised hierarchical clustering, using the top 10% most variant genes based on interquartile range, comparing *PDGFB*-rearranged dermatofibrosarcoma protuberans (n=8, including 3 “conventional” dermatofibrosarcomas protuberans positive for *PDGFB* rearrangement using FISH analysis), *PDGFD*-rearranged dermatofibrosarcoma protuberans (n=9), infantile fibrosarcomas (n=7), clear cell sarcomas of soft tissue (superficially seated) (n=2), *ALK*-rearranged Spitzoid neoplasms (n=5), and *NTRK1/3*-rearranged Spitzoid neoplasms (n=7). Branches depicted with colors within the dendrogram were found significant (p-value < 10e-5) by SigClust clustering significance assessment. Samples are listed in Table 1 and Supplementary Table 4. Infantile fibrosarcomas are highlighted in purple, low grade fibromyxoid sarcomas in orange, spitzoid neoplasms in yellow, clear cell sarcomas in light red and dermatofibrosarcoma protuberans in red.

Alternative *PDGFD* rearrangements in dermatofibrosarcomas protuberans without *PDGFB* fusions

Bérengrère Dadone-Montaudié ^{1*}, Laurent Alberti ^{2,3*}, Adeline Duc ³, Lucile Delespaul ^{4,5#}, Tom Lesluyes ^{4,5#}, Gaelle Perot ⁶, Agnes Lancon ³, Sandrine Paindavoine ³, Ilaria Di Mauro ¹, Jean Yves Blay ^{2,7}, Arnaud de la Fouchardière ³, Frédéric Chibon ^{4,6#}, Marie Karanian ³, Gaëtan MacGrogan ⁶, Valérie Kubiniek ¹, Frédérique Keslair ¹, Nathalie Cardot-Leccia ⁸, Audrey Michot ⁹, Virginie Perrin ¹⁰, Yanis Zekri ¹⁰, Jean-Michel Coindre ^{5,6}, Franck Tirode ^{2,10}, Florence Pedeutour ¹, Dominique Ranchere-Vince ³, François Le Loarer ^{5,6§}, Daniel Pissaloux ^{2,3§}

Authors affiliations

1 Laboratory of Solid Tumors Genetics, Institute for Research on Cancer and Aging of Nice (IRCAN) CNRS UMR 7284/INSERM U1081, Université Côte d'Azur, Centre Hospitalier Universitaire de Nice, Nice, France

2 Univ Lyon, Université Claude Bernard Lyon 1, CNRS 5286, INSERM U1052, Cancer Research Center of Lyon, France

3 Department of Biopathology, Centre Léon Bérard, Lyon, France

4 INSERM U1218 ACTION, Bordeaux, France

5 University of Bordeaux, Bordeaux, France

6 Department of Pathology, Institut Bergonié, Bordeaux, France

7 Department of Oncology, Centre Léon Bérard, Lyon, France

8 Central Laboratory of Pathology, Centre Hospitalier Universitaire de Nice, Nice, France

9 Department of Surgery, Institut Bergonié, Bordeaux, France

10 Department of Translational Research and Innovation, Centre Léon Bérard, Lyon, France

* co-performed the research

current affiliation: INSERM U1037, Cancer Research Center of Toulouse (CRCT), Institut
Claudius Regaud, IUCT-Oncopole, Toulouse, France

§ co-directed the research

Corresponding author

Daniel Pissaloux

Centre Léon Bérard, Department of Pathology, Cheney B, 28 rue Laennec, 69373 Lyon,
France

daniel.pissaloux@lyon.unicancer.fr

Running title

PDGFD rearrangements in dermatofibrosarcoma protuberans

ABSTRACT

Dermatofibrosarcoma protuberans is underlined by recurrent *COL1A1-PDGFB* fusions but approximately 4% of typical dermatofibrosarcoma protuberans remain negative for this translocation in routine molecular screening.

We investigated a series of 21 cases not associated with the pathognomonic *COL1A1-PDGFB* fusion on routine fluorescence in situ hybridization (FISH) testing. All cases displayed morphological and clinical features consistent with the diagnosis of dermatofibrosarcoma protuberans. RNA-sequencing analysis was successful in 20 cases. The classical *COL1A1-PDGFB* fusion was present in 40% of cases (n=8/20), and subsequently confirmed with a *COL1A1* break-apart FISH probe in all but one case (n=7/8). 55% of cases (n=11/20) displayed novel *PDGFD* rearrangements; *PDGFD* being fused either to the 5' part of *COL6A3* (2q37.3) (n=9/11) or *EMILIN2* (18p11) (n=2/11). All rearrangements led to in-frame fusion transcripts and were confirmed at genomic level by FISH and/or array comparative genomic hybridization. *PDGFD*-rearranged dermatofibrosarcoma protuberans presented clinical outcomes similar to typical dermatofibrosarcoma protuberans. Notably, the two *EMILIN2-PDGFD* cases displayed fibrosarcomatous transformation and homozygous deletions of *CDKN2A* at genomic level.

We report the first recurrent molecular variant of dermatofibrosarcoma protuberans involving *PDGFD*, which functionally mimic *bona fide* *COL1A1-PDGFB* fusions, leading presumably to a similar autocrine loop stimulating PDGFRB. This study also emphasizes that *COL1A1-PDGFB* fusions can be cytogenetically cryptic on FISH testing in a subset of cases, thereby representing a diagnostic pitfall that pathologists should be aware of.

Keywords

Dermatofibrosarcoma protuberans; DFSP; *PDGFD*; *COL6A3*; *EMILIN2*; gene fusion; sarcoma.

INTRODUCTION

Dermatofibrosarcoma protuberans is a superficial and locally invasive mesenchymal tumor which undergoes fibrosarcomatous transformation portending a metastatic potential in 10% of cases (1). Giant cell fibroblastoma represents a morphological variant of dermatofibrosarcoma protuberans occurring in children. Both dermatofibrosarcoma protuberans and giant cell fibroblastoma are molecularly defined by the presence of translocation (17;22)(q21.3;q13.1), which fuses *collagen type I alpha 1 chain (COL1A1)* with *platelet-derived growth factor B chain (PDGFB)* (2). Most dermatofibrosarcomas protuberans display typical morphological features including a dense storiform proliferation of cells expressing diffusely and strongly CD34 (1). Fibrous morphological variants of dermatofibrosarcoma protuberans may be confused with benign cellular fibrous histiocytomas or dermatofibromas (1). A diagnosis of dermatofibrosarcoma protuberans warrants complete surgical excision that may require large resection due to the propensity of dermatofibrosarcoma protuberans to infiltrate adjacent tissues (3). Imatinib and pazopanib therapies, which target PDGF downstream signaling, may be used in unresectable or metastatic cases (3,4). Molecular confirmation of dermatofibrosarcoma protuberans is therefore strongly recommended. *COL1A1-PDGFB* fusion gene is mostly screened with dual fusion or break-apart fluorescence *in situ* hybridization (FISH) in routine practice (5). Reverse transcription polymerase chain reaction (RT-PCR) assays are slightly less sensitive than FISH due to the variability of *COL1A1* breakpoints and require non-degraded RNA, although some studies report comparable sensitivity (6,7). Cytogenetic studies have shown that t(17;22) is mostly unbalanced, associated with supernumerary ring chromosomes, and may therefore be evidenced by array comparative genomic hybridization (8,9). Altogether, routine molecular screening remains negative in approximately 4% of otherwise typical dermatofibrosarcomas protuberans, raising clinical uncertainties and leading to render a diagnosis of dermatofibrosarcoma protuberans

lacking the canonical translocation and therefore “molecularly unconfirmed” (5). Single reports of molecular variants of dermatofibrosarcoma protuberans have been reported but no systematic study has been performed so far (10-13).

In order to identify novel fusion genes in dermatofibrosarcoma protuberans, we investigated by RNA-sequencing and array comparative genomic hybridization a series of 21 morphologically typical dermatofibrosarcomas protuberans, negative for *COL1A1-PDGFB* fusion on routine molecular testing.

MATERIALS AND METHODS

Sample selection

We identified 25 cases in our records diagnosed as dermatofibrosarcoma protuberans between 2006 and 2017 but negative on molecular testing. Cases were retrieved from the archives of the department of Genetics of University Hospital of Nice (Nice, France), and departments of Pathology of Centre Léon Bérard (Lyon, France) and Institut Bergonié (Bordeaux, France). Notably, all three participating institutions used FISH for molecular testing, but they applied two different screening strategies. First, *COL1A1-PDGFB* fusion probe followed by *PDGFB* break-apart probe in case of negative or equivocal result. Second, a screening with *PDGFB* break-apart probe in the first place, followed if negative or ambiguous by a screening with a *COL1A1* break-apart probe. Due to the evolution of molecular testing strategies over time, 7 cases of our series had not been previously tested with a *PDGFB* break apart probe. Hence, FISH analysis was completed in these cases, rendering positive results in 4 cases, which were therefore removed from the final cohort (n=21).

All cases from the series were registered in the RREPS sarcoma database, a national clinical database approved by the Commission Nationale Informatique et Libertés (CNIL) and the Comité national d'éthique.

The material used in this publication was provided by the SarcomaBCB, the Conticanet database (<https://auth.sarcomabcb.org>).

Clinical review

Clinical follow-up was obtained from the medical records of patients either available at our institutions or through corresponding clinicians. Follow-up duration was calculated from the date of the clinical detection of the lesion. Clinical data are provided in **Supplementary Table 1**.

Histopathological analyses

All cases of the final series were reviewed blindly by soft tissue expert pathologists (FLL, JMC, DRV). Fibrosarcomatous transformation was defined by the presence of a fascicular component with increased mitotic activity contrasting with the storiform pattern of the DFSP component (1). All samples were studied with a panel of antibodies available in routine including AE1/E3, CD34, S100 protein, EMA, and Ki67. Pathological data are summarized in **Supplementary Table 1**.

Fluorescence in situ hybridization (FISH) analyses

FISH analyses were performed on formalin-fixed paraffin-embedded tissue sections using commercial and custom bacterial artificial chromosome (BAC) probes. Commercial FISH probes used in the study included dual fusion probe *COL1A1/PDGFB* (#Z-2116-200, Zytovision, Bremerhaven, Germany), *PDGFB* Break Apart probe (#Z-2119-200, Zytovision), and *COL1A1* Break Apart Probe (#Z-2121-200, ZytoVision). *PDGFD*, *EMILIN2* and *COL6A3* break-apart probes were prepared with BAC listed in **Supplementary Table 2**. FISH analysis was performed by assessing at least 100 non-overlapping intact nuclei by two independent operators. The positive threshold to call the FISH assay positive was 15%. BACs were cultured and labelled as previously described (14).

Array Comparative Genomic Hybridization analyses

Genomic DNA was extracted from formalin-fixed paraffin-embedded tissue using QIAamp, DNA micro kit (Qiagen, Hilden, Germany). Genomic DNA and human reference DNA (Promega) were labeled with cyanin 5 (Cy5) and cyanine 3 (Cy3), respectively, using the Genomic DNA High-Throughput *ULS* Labeling Kit (Agilent Technologies, Santa Clara, California) and co-hybridized onto a Sureprint G3 Human CGH microarray 4x180K (Agilent) following manufacturer's recommendations. Data were analyzed by Agilent Genomic Workbench software v7.0 or by Cytogenomics software (v2.9.2.4, Agilent) and expressed according to the human reference hg19 (GRCh37, Genome Reference Consortium Human Reference 37). The identification of aberrant copy number segments was based on ADM-2 segmentation algorithm with a threshold of 6.0.

RNA-sequencing analyses

RNA sequencing was performed with formalin-fixed paraffin-embedded material in all cases. Total RNA was extracted from formalin-fixed paraffin-embedded tissue section using Trizol reagent (Thermo Fisher Scientific, Courtaboeuf, France) following manufacturers' recommendations. DNA was removed using RNase-free DNase set (Qiagen) followed by second Trizol extraction. Quantity and quality of total RNA were evaluated using NanoDrop (Thermo Fisher Scientific) and Tape Station with Hs RNA Screen Tape (Agilent) using a cut off of DV₂₀₀ (defined as the percentage of RNA fragments above 200 nucleotides) above 13%. All samples passed quality criteria. Libraries were prepared with 100 ng of total RNA using TruSeq RNA Access Library Prep Kit (Illumina, San Diego, USA). Libraries were pooled by group of 14 samples at 4 nM with 1% PhiX. Sequencing was performed (75 cycles paired end) using a NextSeq 500/550 High Output V2 kit on Illumina NextSeq 500 platform (Illumina, San Diego, CA). RNA-sequencing was successful in 20 out of 21 cases. The case with failure was ruled out from the final series as no material was available to complete its

characterization by array comparative genomic hybridization and FISH (final series n=20, **Table 1**).

Sequencing data (up to 15 million reads per sample) were analyzed with BaseSpace sequence Hub (Illumina). Reads were aligned with STAR and TopHat2 on GRCh 38 reference genome. The fusion transcripts were called with Manta, STAR-Fusion, FusionMap and TopHat2 fusion and validated if the Manta score was up to 0.7 and present in fusion list with TopHat2 fusion and/or STAR-Fusion and/or FusionMap (15-17).

To perform the clustering analysis, gene expression values were extracted using Kallisto v0.42.5 tool (18) with GENECODE release 23 genome annotation based on GRCh38 genome reference. Kallisto TPM expression values were transformed in $\log_2(\text{TPM}+2)$ and all samples were normalized together using the quantile method from the R limma package within R (version 3.1.1) environment. Clustering was performed with the R package Cluster v2.0.3 using Pearson correlation distance and Ward's clustering method. Significance of clusters was assessed using SigClust as previously described (19).

Reverse transcriptase-polymerase chain reaction (RT-PCR) and Sanger sequencing

In 11 cases, we performed RT-PCR to confirm either the *COL6A3-PDGFD* fusion transcript or the *EMILIN2-PDGFD* fusion transcript, using the following custom primers (designed using Primer 3 program): *COL6A3* forward primer 5'GCAAGGTCAGCTTCTAGTTCA3', *PDGFD* reverse primer 5'TGGCCAACCTTCAGCTCTTCT3' (in case number 1, 2, 4, 5, 6, 7, 8, 19), *COL6A3* forward primer 5'CAGCAAGGTCAGCTTCTAGTT3' and *PDGFD* reverse primer 5'CAGTTCCACAGCCACAATTTTC3' (in case number 3) and *EMILIN2* forward primer 5'GCCACGTCTTCCAGATTTCTA3' and *PDGFD* reverse primer 5'CAGTTCCACAGCCACAATTTTC3' (in case number 9, 10). Fusion transcripts were sequenced by Sanger after extraction and enzymatic purification of RT-PCR product using High pure PCR product purification kit (Roche Diagnostics, Meylan, France).

RESULTS

Clinicopathological features

All cases were located in classical anatomical sites including trunk (n=11/20), limbs (n=6/20) and head and neck (n=3/20) (**Table 1**). Patients' age ranged from 4 to 73 years old. Clinically, lesions presented with a classical scar-like appearance (n=2), slow-growing cutaneous plaques (n=1) or cutaneous plaques with red discoloration (n=2). Additionally, one case had a multinodular presentation. All tumors displayed outcomes in line with the local malignant potential of dermatofibrosarcoma protuberans with late local recurrences occurring up to 12 years after initial resection (Supplementary Table 1). All cases presented morphological features either typical of dermatofibrosarcoma protuberans (n=12/20) (**Figure 1 and 2**) or consistent with a morphological variant of dermatofibrosarcoma protuberans including fibrous pattern (n=5/20), pigmented pattern (also referred to as Bednar tumor) (n=1/20) or hybrid Bednar/ dermatofibrosarcoma protuberans variant with focal presence of pigments or giant cells (n=2/20) (**Supplementary Table 1**). Four cases displayed fibrosarcomatous transformation (**Figure 3**). All but two cases showed classical honeycomb infiltrative borders. Five cases were deeply located in hypodermis without dermal infiltration.

RNA-sequencing

Classical *COL1A1-PDGFB* fusions were found in 8 cases (n=8/20). *PDGFB* breakpoint was constantly found in exon 2 while breakpoints in *COL1A1* varied from exons 11 to 45 (**Supplementary Table 3**).

PDGFD rearrangements were found in eleven cases (n=11/20), *PDGFD* being fused either to collagen type VI alpha 3 chain (*COL6A3*) at 2q37 (n=9/11) or elastin microfibril Interface 2 (*EMILIN2*) at 18p11 (n=2/11). Breakpoints in *COL6A3* involved either exon 42 (n=8/9) or

exon 43 (n=1/9), while breakpoint in *PDGFD* constantly involved exon 6 (**Figure 2**) and breakpoints in *EMILIN2* were located within exon 4 (**Figure 3**).

One case (case number 20) failed to show a fusion transcript by RNA-sequencing with the different algorithms.

FISH and RT-PCR

COL6A3-PDGFD transcript and *EMILIN2-PDGFD* transcript were confirmed by RT-PCR in all cases (case number 1-10 and 19). Regarding cases with *COL1A1-PDGFB* fusions, FISH analyses were completed with a *COL1A1* break-apart probe, which was positive in 7/8 cases (**Figure 1**). Regarding cases with *PDGFD* fusions, FISH analyses were carried out with *PDGFD* break-apart probe which was positive in 9 cases out of 11 (n=9/11). Gene partners fused to *PDGFD* were also assessed with *COL6A3* and *EMILIN2* break-apart probes (**Figure 2** and **3**, respectively), showing rearrangements in 5/7 and 2/2 cases, respectively (**Supplementary Table 3**).

Array comparative genomic hybridization

On profiles, all cases with cryptic *COL1A1-PDGFB* highlighted genomic breakpoints within *COL1A1* with a genomic gain in flanking region 17q21.33-qter (n=5/5). Additional non-recurrent copy number alterations were present in all cases. Genomic gains were seen in 1q21-q25.3, 4q28-q35, 6p, 7pter, 22q11 in one case each. Whole chromosome gains involved chromosomes 6, 7, 10 and genomic loss were seen in 1q22-23 6q12-q26 and 8p in one case each (**Supplementary Table 3**).

Array comparative genomic hybridization analysis of the dermatofibrosarcomas protuberans with *COL6A3-PDGFD* fusion highlighted no breakpoint within *PDGFB* nor *COL1A1* but within *COL6A3* and *PDGFD* in 4/7 and 6/8 cases, respectively. Copy number alterations were present in the regions flanking the breakpoints in all but one case (n=6/7). Additional non-recurrent copy number alterations included gain of chromosome 12 (n=1/7), loss of 3q

(n=1/7), gains of chromosomes 1, 7 and 17 (n=1/7). The genomic profiles of the 2 cases of *EMILIN2-PDGFD* dermatofibrosarcoma protuberans displayed breakpoints within *PDGFD* (n= 1/2), without copy number alteration involving *EMILIN2*. Interestingly, both profiles presented homozygous deletion of *CDKN2A* locus (n=2/2). None of these cases displayed copy number alterations in the genomic regions flanking the breakpoints.

Clustering analysis

To assess whether *PDGFD*-rearranged dermatofibrosarcoma protuberans were biologically similar to *PDGFB*-rearranged dermatofibrosarcoma protuberans, we compared the RNA-seq expression profiles of samples of our cohort (including 5 *PDGFB*- and 9 *PDGFD*-rearranged dermatofibrosarcoma protuberans) to other spindled cutaneous neoplasms including infantile fibrosarcomas (n=7), clear cell sarcomas of soft tissue (n=2), *ALK*-rearranged Spitzoid neoplasms (n=5), *NTRK1/3*-rearranged Spitzoid neoplasms (n=7) and conventional *PDGFB*-rearranged dermatofibrosarcomas protuberans positive for gene rearrangement upon routine molecular screening (n= 3) (**Supplementary Table 4**). All cases clustered together with transcriptional profiles distinct from *ALK*- and *NTRK1/3*-rearranged Spitzoid proliferations and infantile fibrosarcomas. The dermatofibrosarcoma protuberans cluster lumped together all dermatofibrosarcoma protuberans including those with *PDGFB* fusions (both cryptic and overt rearrangements) and *PDGFD* fusions (**Figure 4**).

DISCUSSION

Dermatofibrosarcoma protuberans has historically been defined by the presence of recurrent *COL1A1-PDGFB* fusions which lead to the upregulation of PDGFRB signaling through an autocrine activating loop (20-23). However, approximately 4% of dermatofibrosarcoma protuberans prove negative for the translocation upon routine FISH testing (5).

We evidenced by RNA-sequencing that molecularly unconfirmed dermatofibrosarcoma protuberans displayed “cryptic” *COL1A1-PDGFB* fusions in 40% of cases (n=8/20). All dermatofibrosarcomas protuberans associated with “cryptic” fusions involved previously reported *COL1A1* breakpoints which position have been shown to vary considerably from exon 7 to exon 49. Interestingly, all cases displayed visible genomic breakpoints within *COL1A1* on quantitative genomic profiles along with and/or gains of the 17q locus flanking the breakpoint (n=5/5) (**Figure 1**). Notably, subsequent FISH analyses with *COL1A1* break-apart probe were positive in all but one case (n=7/8). Altogether, our findings support that array comparative genomic hybridization or screening with *COL1A1* break-apart probe may support the diagnosis of cryptic dermatofibrosarcoma protuberans. This complementary screening strategy remains cost-effective as compared to the cost of RNA-sequencing performed in all cases suspicious of dermatofibrosarcoma protuberans. Cryptic rearrangements have also been reported in other translocation-related sarcomas and are thought to be related to structural variations of the translocation or induction of neo-exons secondary to splicing variations (24-28).

Secondly, we report herein that 55% (n=11/20) of cytogenetically negative-dermatofibrosarcoma protuberans are associated with alternative rearrangements involving *PDGFD*. Two different types of fusion transcripts were evidenced with the 3' part of *PDGFD* being fused to the 5' part either of *COL6A3* (n=9/11) or *EMILIN2* (n=2/11). *PDGFD*, located at 11q22.3, encodes a protein belonging to the same family of *platelet-derived growth factor* than *PDGFB* (29). *PDGFD* is able to bind to PDGF receptor B (*PDGFRB*) (30,31). *PDGFD* has oncogenic properties through promotion of cell proliferation and angiogenesis (29) and its overexpression has been linked to a variety of malignancies (32-35). The breakpoint was constantly located within exon 6, preserving the binding domain to PDGF receptors in a similar manner than translocations involving *PDGFB*. Interestingly, the loss of exon 6 have

been shown to induce truncation due to a premature stop codon in mice, therefore a breakpoint located downstream exon 6 might jeopardize PDGFD signaling (36). *COL6A3*, located at 2q37.3, encodes a protein of extracellular matrix involved in cellular adhesion belonging to the same superfamily as *COL1A1* (37). *COL6A3* contains 3152 amino acids-long alpha3 chains which have the same sequence as alpha1 chains and harbor the same triple-helical and von Willebrand factor A domains (37). Notably, somatic rearrangements of *COL6A3* have been previously reported in tenosynovial giant cell tumors in which *COL6A3* is fused to *Colony Stimulating Factor 1 (CSF1)* (38,39). In addition, overexpression of *COL6A3* has been described in a wide array of malignancies including gastric (40), ovarian (41), colorectal (42,43) and pancreatic cancers (44). It has also been correlated to resistance to chemotherapy (41,45). The breakpoint occurred in exon 42 of *COL6A3* in all but one case (n=8/9), in contrast to the frequent variations seen in *COL1A1*. All *COL6A3-PDGFD* cases displayed genomic imbalances in regions flanking the breakpoints of *COL6A3* and/or *PDGFD* and three cases displayed additional copy number alterations (n=3/7). The morphological and clinical features of *COL6A3*-rearranged dermatofibrosarcoma protuberans did not differ from those seen in *bona fide* dermatofibrosarcoma protuberans. The second fusion partner *EMILIN2* was involved in 2/11 cases a. *EMILIN2*, located at 18p11.32-p11.31, encodes a glycoprotein related to the superfamily of collagen which contains collagen-like domains (37). *EMILIN2* assembles into multimers, involved in the composition of extracellular matrix (46,47). The genomic breakpoints were located constantly in exons 4 and 6 of *EMILIN2* and *PDGFD*, respectively. The fusion preserved preserves key structural domains of *EMILIN2*, including EMI domain, coiled-coil structures and leucine zippers and gC1q domain (46,47). *EMILIN2-PDGFD* dermatofibrosarcoma protuberans displayed homozygous deletion of *CDKN2A* in both cases (n=2/2). Interestingly, both cases displayed fibrosarcomatous transformation and were deep-seated within hypodermis without dermal

connection. It is notable that homozygous deletions of *CDKN2A* are linked to malignancy in varied tumor types including mesenchymal, melanocytic and epithelial neoplasms (48-50). Therefore, this alteration may portend an increased malignant potential in this subset of dermatofibrosarcoma protuberans which warrants further studies on larger cohorts with longer follow-up to assess whether the behavior of cases of *EMILIN2-PDGFD* dermatofibrosarcoma protuberans is similar or not to classical and *COL6A3-PDGFD*-associated cases.

Altogether, *PDGFD* rearrangements may functionally mimic the biology of *COL1A1-PDGFB* fusions as it involves functionally related genes and display a similar structure. Rearrangements might therefore be targeted by imatinib as classical dermatofibrosarcoma protuberans.

In conclusion, we report herein new and recurrent molecular variants of dermatofibrosarcoma protuberans underlined by *PDGFD* rearrangements, which are clinically, morphologically and molecularly indistinguishable from *COL1A1-PDGFB* dermatofibrosarcoma protuberans. Furthermore, we showed that roughly half of cases of dermatofibrosarcoma protuberans negative upon routine FISH screening are associated with cryptic *COL1A1-PDGFB* rearrangements that may be identified by array comparative genomic hybridization or FISH with a *COL1A1* break-apart probe. The functional similarities between the classical *COL1A1-PDGFB* and the alternative *COL6A3-PDGFD* or *EMILIN2-PDGFD* transcripts suggest they activate an analogous oncogenic autocrine loop involving PDGFRB signaling.

Acknowledgements

The authors wish to thank pathologists and clinicians who provided samples and clinical follow-up: M Chargeboeuf (Lons le Saunier), C Charon-Barra (Dijon), C Delfour (Montpellier), S Depardieu (Metz), A Leroux (Vandoeuvre les Nancy), A Lipandy (Nimes), E

Maubec (Paris), C de Mauroy (Rouen), YM Robin (Lille), JF Totton (Besancon), M Battistella (Paris) and MP Wissler (Villeurbanne). The authors are grateful for their insights and participation in this study to A Bazin, AC Peyron and A Ribeiro.

This work was supported by grants from La Ligue contre le Cancer de l'Ain et de Savoie, Institut National du Cancer (NETSARC, RREPS, RESOS).

Disclosure / Conflict of Interest

The authors declare no conflict of interest.

Supplementary information is available at Modern Pathology's website.

References

- 1 Mentzel T, Pedeutour F, Lazar A and Coindre JM. Dermatofibrosarcoma protuberans. In: Fletcher CDM, Bridge JA, Hogendoorn PCW and Mertens, editors. WHO classification of tumours of soft tissue and bone. 4th ed. Lyon: IARC, 2013. p.77-79
- 2 Simon MP, Pedeutour F, Sirvent N, et al. Deregulation of the platelet-derived growth factor B-chain gene via fusion with collagen gene COL1A1 in dermatofibrosarcoma protuberans and giant-cell fibroblastoma. *Nat Genet* 1997;15:95-98
- 3 Saiag P, Grob J-J, Lebbe C, et al. Diagnosis and treatment of dermatofibrosarcoma protuberans. European consensus-based interdisciplinary guideline. *Eur J Cancer* 2015;51:2604-2608
- 4 Stacchiotti S, Pantaleo MA, Negri T, et al. Efficacy and Biological Activity of Imatinib in Metastatic Dermatofibrosarcoma Protuberans (DFSP). *Clin Cancer Res* 2016;22:837-846
- 5 Karanian M, Pérot G, Coindre J-M, et al. Fluorescence in situ hybridization analysis is a helpful test for the diagnosis of dermatofibrosarcoma protuberans. *Mod Pathol* 2015;28:230-237
- 6 Salgado R, Llombart B, M Pujol R, et al. Molecular diagnosis of dermatofibrosarcoma protuberans: a comparison between reverse transcriptase-polymerase chain reaction and fluorescence in situ hybridization methodologies. *Genes Chromosomes Cancer* 2011;50:510-517
- 7 Patel KU, Szabo SS, Hernandez VS, et al. Dermatofibrosarcoma protuberans COL1A1-PDGFB fusion is identified in virtually all dermatofibrosarcoma protuberans cases when investigated by newly developed multiplex reverse transcription polymerase chain reaction and fluorescence in situ hybridization assays. *Hum Pathol* 2008;39:184-193
- 8 Linn SC, West RB, Pollack JR, et al. Gene expression patterns and gene copy number

- changes in dermatofibrosarcoma protuberans. *Am J Pathol* 2003;163:2383-2395
- 9 Sirvent N, Maire G, Pedeutour F. Genetics of dermatofibrosarcoma protuberans family of tumors: from ring chromosomes to tyrosine kinase inhibitor treatment. *Genes Chromosomes Cancer* 2003;37:1-19
- 10 Nakamura I, Kariya Y, Okada E, et al. A Novel Chromosomal Translocation Associated With COL1A2-PDGFB Gene Fusion in Dermatofibrosarcoma Protuberans: PDGF Expression as a New Diagnostic Tool. *JAMA Dermatol* 2015;151:1330-1337
- 11 Bianchini L, Maire G, Guillot B, et al. Complex t(5;8) involving the CSPG2 and PTK2B genes in a case of dermatofibrosarcoma protuberans without the COL1A1-PDGFB fusion. *Virchows Arch Int J Pathol* 2008;452:689-696
- 12 Saab J, Rosenthal IM, Wang L, et al. Dermatofibrosarcoma Protuberans-Like Tumor With COL1A1 Copy Number Gain in the Absence of t(17;22). *Am J Dermatopathol* 2017;39:304-309
- 13 Sinovic J, Bridge JA. Translocation (2;17) in recurrent dermatofibrosarcoma protuberans. *Cancer Genet Cytogenet.* 1994;75:156-7.
- 14 Sirvent N, Coindre J-M, Maire G, et al. Detection of MDM2-CDK4 amplification by fluorescence in situ hybridization in 200 paraffin-embedded tumor samples: utility in diagnosing adipocytic lesions and comparison with immunohistochemistry and real-time PCR. *Am J Surg Pathol* 2007;31:1476-1489
- 15 Trapnell C, Roberts A, Goff L, et al. Differential gene and transcript expression analysis of RNA-seq experiments with TopHat and Cufflinks. *Nat Protoc* 2012;7:562-578
- 16 Ge H, Liu K, Juan T, et al. FusionMap: detecting fusion genes from next-generation sequencing data at base-pair resolution. *Bioinforma Oxf Engl* 2011;27:1922-1928
- 17 Lågstad S, Zhao S, Hoff AM, et al. chimeraviz: a tool for visualizing chimeric RNA. *Bioinforma Oxf Engl* 2017;33:2954-2956

- 18 Bray NL, Pimentel H, Melsted P, et al. Near-optimal probabilistic RNA-seq quantification. *Nat Biotechnol* 2016;34:525-527
- 19 Le Loarer F, Watson S, Pierron G, et al. SMARCA4 inactivation defines a group of undifferentiated thoracic malignancies transcriptionally related to BAF-deficient sarcomas. *Nat Genet* 2015;47:1200-1205
- 20 Simon MP, Pedeutour F, Sirvent N, et al. Deregulation of the platelet-derived growth factor B-chain gene via fusion with collagen gene COL1A1 in dermatofibrosarcoma protuberans and giant-cell fibroblastoma. *Nat Genet* 1997;15:95-98
- 21 Greco A, Fusetti L, Villa R, et al. Transforming activity of the chimeric sequence formed by the fusion of collagen gene COL1A1 and the platelet derived growth factor b-chain gene in dermatofibrosarcoma protuberans. *Oncogene* 1998;17:1313-1319
- 22 Shimizu A, O'Brien KP, Sjöblom T, et al. The dermatofibrosarcoma protuberans-associated collagen type Ialpha1/platelet-derived growth factor (PDGF) B-chain fusion gene generates a transforming protein that is processed to functional PDGF-BB. *Cancer Res* 1999;59:3719-3723
- 23 Sjöblom T, Shimizu A, O'Brien KP, et al. Growth inhibition of dermatofibrosarcoma protuberans tumors by the platelet-derived growth factor receptor antagonist STI571 through induction of apoptosis. *Cancer Res* 2001;61:5778-5783
- 24 Brassesco MS, Cortez MA, Valera ET, et al. Cryptic SYT/SXX1 fusion gene in high-grade biphasic synovial sarcoma with unique complex rearrangement and extensive BCL2 overexpression. *Cancer Genet Cytogenet* 2010;196:189-193
- 25 Torres L, Lisboa S, Cerveira N, et al. Cryptic chromosome rearrangement resulting in SYT-SSX2 fusion gene in a monophasic synovial sarcoma. *Cancer Genet Cytogenet* 2008;187:45-49
- 26 Lestou VS, O'Connell JX, Robichaud M, et al. Cryptic t(X;18), ins(6;18), and SYT-

- SSX2 gene fusion in a case of intraneural monophasic synovial sarcoma. *Cancer Genet Cytogenet* 2002;138:153-156
- 27 Kovar H, Jugovic D, Melot T, et al. Cryptic exons as a source of increased diversity of Ewing tumor-associated EWS-FLI1 chimeric products. *Genomics* 1999;60:371-374
- 28 Chen S, Deniz K, Sung Y-S, et al. Ewing sarcoma with ERG gene rearrangements: A molecular study focusing on the prevalence of FUS-ERG and common pitfalls in detecting EWSR1-ERG fusions by FISH. *Genes Chromosomes Cancer* 2016;55:340-349
- 29 Wang Z, Kong D, Li Y, et al. PDGF-D signaling: a novel target in cancer therapy. *Curr Drug Targets* 2009;10:38-41
- 30 Bergsten E, Uutela M, Li X, et al. PDGF-D is a specific, protease-activated ligand for the PDGF beta-receptor. *Nat Cell Biol* 2001;3:512-516
- 31 LaRochelle WJ, Jeffers M, McDonald WF, et al. PDGF-D, a new protease-activated growth factor. *Nat Cell Biol* 2001;3:517-521
- 32 Torres-Martin M, Lassaletta L, Isla A, et al. Global expression profile in low grade meningiomas and schwannomas shows upregulation of PDGFD, CDH1 and SLIT2 compared to their healthy tissue. *Oncol Rep* 2014;32:2327-2334
- 33 Ustach CV, Kim H-RC. Platelet-derived growth factor D is activated by urokinase plasminogen activator in prostate carcinoma cells. *Mol Cell Biol* 2005;25:6279-6288
- 34 Wang Z, Kong D, Banerjee S, et al. Down-regulation of platelet-derived growth factor-D inhibits cell growth and angiogenesis through inactivation of Notch-1 and nuclear factor-kappaB signaling. *Cancer Res* 2007;67:11377-11385
- 35 Xu L, Tong R, Cochran DM, et al. Blocking platelet-derived growth factor-D/platelet-derived growth factor receptor beta signaling inhibits human renal cell carcinoma progression in an orthotopic mouse model. *Cancer Res* 2005;65:5711-5719
- 36 Reigstad LJ, Varhaug JE, Lillehaug JR. Structural and functional specificities of

PDGF-C and PDGF-D, the novel members of the platelet-derived growth factors family.

FEBS J 2005;272:5723-5741

37 Ricard-Blum S. The collagen family. Cold Spring Harb Perspect Biol 2011;3:a004978

38 West RB, Rubin BP, Miller MA, et al. A landscape effect in tenosynovial giant-cell tumor from activation of CSF1 expression by a translocation in a minority of tumor cells.

Proc Natl Acad Sci U S A 2006;103:690-695

39 Möller E, Mandahl N, Mertens F, et al. Molecular identification of COL6A3-CSF1 fusion transcripts in tenosynovial giant cell tumors. Genes Chromosomes Cancer 2008;47:21-25

40 Xie X, Liu X, Zhang Q, et al. Overexpression of collagen VI $\alpha 3$ in gastric cancer.

Oncol Lett 2014;7:1537-1543

41 Sherman-Baust CA, Weeraratna AT, Rangel LBA, et al. Remodeling of the extracellular matrix through overexpression of collagen VI contributes to cisplatin resistance in ovarian cancer cells. Cancer Cell 2003;3:377-386

42 Qiao J, Fang C-Y, Chen S-X, et al. Stroma derived COL6A3 is a potential prognosis marker of colorectal carcinoma revealed by quantitative proteomics. Oncotarget

2015;6:29929-29946

43 Yu J, Wu WKK, Li X, et al. Novel recurrently mutated genes and a prognostic mutation signature in colorectal cancer. Gut 2015;64:636-645

44 Arafat H, Lazar M, Salem K, et al. Tumor-specific expression and alternative splicing of the COL6A3 gene in pancreatic cancer. Surgery 2011;150:306-315

45 Park J, Morley TS, Scherer PE. Inhibition of endotrophin, a cleavage product of collagen VI, confers cisplatin sensitivity to tumours. EMBO Mol Med 2013;5:935-948

46 Mongiat M, Mungiguerra G, Bot S, et al. Self-assembly and supramolecular organization of EMILIN. J Biol Chem 2000;275:25471-25480

- 47 Colombatti A, Spessotto P, Doliana R, et al. The EMILIN/Multimerin family. *Front Immunol* 2011;2:93
- 48 Hwang HC, Sheffield BS, Rodriguez S, et al. Utility of BAP1 Immunohistochemistry and p16 (CDKN2A) FISH in the Diagnosis of Malignant Mesothelioma in Effusion Cytology Specimens. *Am J Surg Pathol* 2016;40:120-126
- 49 Li Z, Gonzalez CL, Wang B, et al. Cdkn2a suppresses metastasis in squamous cell carcinomas induced by the gain-of-function mutant p53(R172H). *J Pathol* 2016;240:224-234
- 50 Rebouissou S, Hérault A, Letouzé E, et al. CDKN2A homozygous deletion is associated with muscle invasion in FGFR3-mutated urothelial bladder carcinoma. *J Pathol* 2012;227:315-324

Figure legends

Figure 1. Cryptic *COL1A1-PDGFB* fusion in dermatofibrosarcoma protuberans. A-B.

Band-like infiltration of hypodermis and subcutaneous adipose tissue (case number 15, HES staining, x2,5 and X6,5 magnifications, respectively) **C.** Storiform proliferation infiltrating hypodermis with a honeycomb pattern (HES, X200 magnification). **D-E.** High power field view of tumour cell nuclei displaying ovoid shape and monomorphism (**D**) and focal interspersed multinucleated cells (**E**) (HES, X200 magnification) **F.** Fluorescence *in situ* hybridization (FISH) using *COL1A1* break-apart probe. FISH analysis shows an unbalanced translocation with a gain of the 5' part of *COL1A1* (probe labelled in red). **G.** Array-comparative genomic hybridization profile harbors a genomic breakpoint at *COL1A1* locus with a 5' *COL1A1* gain but no breakpoint at *PDGFB* locus (chromosome 22 view not shown). Additional copy number alterations include gains of 4q28-q35, 6p and whole chromosome 7.

Figure 2. *COL6A3-PDGFD* dermatofibrosarcoma protuberans. A.

Biopsy specimen highlighting deep-seated dense nodular proliferation (case number 6, HES staining, X20 magnification). **B.** Storiform proliferation with honeycomb infiltrative pattern typical of dermatofibrosarcoma protuberans (HES, X200). **C.** Fibrous stromal changes focally interposed between tumor cells (HES, X250) **D.** Tumor cells display ovoid monomorphic nuclei (HES, X400). **E** Array-comparative genomic hybridization profile showing deletions and breakpoints involving *COL6A3* and *PDGFD*. Additional copy number alteration includes gain of chromosome 12. **F-G.** Fluorescence *in situ* hybridization (FISH) using *COL6A3* break-apart probe (**F**) and *PDGFD* break-apart probe (**G**) showing an unbalanced rearrangement with loss of the 3' *COL6A3* and the 5' *PDGFD*, respectively. **H.** Structure of *COL6A3-PDGFD* fusion transcript. From top to bottom: scheme representing locus and chromosomal position of *COL6A3* and *PDGFD*; schematic of breakpoints positions involving *COL6A3* exon 42 and *PDGFD* exon 6; nucleotide sequence of adjoined sequences.

Figure 3. *EMILIN2-PDGFD* dermatofibrosarcoma protuberans. **A.** Biopsy specimen highlighting densely cellular tumor infiltrating hypodermis (case number 9, HES staining, X2 magnification). **B.** Focal collagenized stroma arranged in elongated fascicles suspicious for fibrosarcomatous transformation (X200 magnification). **C.** Tumor cells display ovoid monomorphic nuclei embedded in a collagenous stroma (X400 magnification). **D.** CD34 staining in this case (X250 magnification). **E.** Array-comparative genomic hybridization profile showing a homozygous deletion of *CDKN2A* (P16) but no breakpoint within *EMILIN2* or *PDGFD* loci. **F-G.** Fluorescence *in situ* hybridization (FISH) using *EMILIN2* break-apart probe (**F**) and *PDGFD* break-apart probe (**G**) showing a rearrangement of the *EMILIN2* and *PDGFD* loci, respectively. **H.** Structure of *EMILIN2-PDGFD* fusion. From top to bottom scheme representing locus and chromosomal position of *EMILIN2* and *PDGFD*; schematic of breakpoints positions which constantly occurred in exon 4 of *EMILIN2* and in exon 6 of *PDGFD*; nucleotide sequence of adjoined sequences.

Figure 4. Transcriptomic classification of dermatofibrosarcoma protuberans.

Unsupervised hierarchical clustering, using the top 10% most variant genes based on interquantile range, comparing *PDGFB*-rearranged dermatofibrosarcoma protuberans (n=8, including 3 “conventional” dermatofibrosarcomas protuberans positive for *PDGFB* rearrangement using FISH analysis), *PDGFD*-rearranged dermatofibrosarcoma protuberans (n=9), infantile fibrosarcomas (n=7), clear cell sarcomas of soft tissue (superficially seated) (n=2), *ALK*-rearranged Spitzoid neoplasms (n=5), and *NTRK1/3*-rearranged Spitzoid neoplasms (n=7). Branches depicted with colors within the dendrogram were found significant (p-value < 10e-5) by SigClust clustering significance assessment. Samples are listed in Table 1 and Supplementary Table 4. Infantile fibrosarcomas are highlighted in purple, low grade fibromyxoid sarcomas in orange, spitzoid neoplasms in yellow, clear cell sarcomas in light red and dermatofibrosarcoma protuberans in red.

Case number	Age (years)/ Gender	Location	Diagnosis	RNA Sequencing	Array-comparative genomic hybridization	FISH validation	RT-PCR validation
1	33/M	Abdominal wall	Dermatofibrosarcoma protuberans	<i>COL6A3-PDGFD</i> fusion	<i>COL6A3</i> breakpoint: 3' <i>COL6A3</i> heterozygous deletion	Split <i>PDGFD</i> : + Split <i>COL6A3</i> : +	<i>COL6A3-PDGFD</i> fusion
2	38/F	Breast	Dermatofibrosarcoma protuberans	<i>COL6A3-PDGFD</i> fusion	<i>PDGFD</i> breakpoint: <i>PDGFD</i> intragenic deletion	Split <i>PDGFD</i> : + Split <i>COL6A3</i> : +	<i>COL6A3-PDGFD</i> fusion
3	38/F	Chest wall	Dermatofibrosarcoma protuberans	<i>COL6A3-PDGFD</i> fusion	<i>PDGFD</i> breakpoint: <i>PDGFD</i> intragenic deletion	Split <i>PDGFD</i> : + Split <i>COL6A3</i> : +	<i>COL6A3-PDGFD</i> fusion
4	48/F	Chest wall	Dermatofibrosarcoma protuberans	<i>COL6A3-PDGFD</i> fusion	<i>COL6A3</i> breakpoint: 3' <i>COL6A3</i> heterozygous deletion <i>PDGFD</i> breakpoint: <i>PDGFD</i> intragenic deletion	Split <i>PDGFD</i> : Failure Split <i>COL6A3</i> : Failure	<i>COL6A3-PDGFD</i> fusion
5	33/F	Shoulder	Dermatofibrosarcoma protuberans	<i>COL6A3-PDGFD</i> fusion	<i>COL6A3</i> breakpoint: 3' <i>COL6A3</i> heterozygous deletion <i>PDGFD</i> breakpoint: 5' <i>PDGFD</i> heterozygous deletion	ND	<i>COL6A3-PDGFD</i> fusion
6	39/F	Back	Dermatofibrosarcoma protuberans	<i>COL6A3-PDGFD</i> fusion	<i>COL6A3</i> breakpoint: 3' <i>COL6A3</i> heterozygous deletion <i>PDGFD</i> breakpoint: 5' <i>PDGFD</i> heterozygous deletion	Split <i>PDGFD</i> : + Split <i>COL6A3</i> : +	<i>COL6A3-PDGFD</i> fusion

7	29/F	Breast	Dermatofibrosarcoma protuberans	<i>COL6A3-PDGFD</i> fusion	Failure	Split <i>PDGFD</i> : + Split <i>COL6A3</i> : +	<i>COL6A3-PDGFD</i> fusion
8	41/F	Chest wall	Dermatofibrosarcoma protuberans	<i>COL6A3-PDGFD</i> fusion	ND	Split <i>PDGFD</i> : + Split <i>COL6A3</i> : + Failure	<i>COL6A3-PDGFD</i> fusion
9	21/F	Leg	Fibrosarcoma	<i>EMILIN2-PDGFD</i> fusion <i>COL5A1-UBAP1L</i> fusion	No breakpoint within <i>PDGFD</i> or <i>EMILIN2</i>	Split <i>PDGFD</i> : + Split <i>EMILIN2</i> : +	<i>EMILIN2-PDGFD</i> fusion
10	50/M	Leg	Fibrosarcoma	<i>EMILIN2-PDGFD</i> fusion	<i>PDGFD</i> breakpoint: <i>PDGFD</i> intragenic deletion	Split <i>PDGFD</i> : + Split <i>EMILIN2</i> : +	<i>EMILIN2-PDGFD</i> fusion
11	64/M	Back	Atypical dermatofibrosarcoma protuberans	<i>COL1A1-PDGFB</i> fusion	<i>COL1A1</i> breakpoint: 5' <i>COL1A1</i> gain	Split <i>COL1A1</i> : +	
12	24/M	Thigh	Fibrosarcoma	<i>COL1A1-PDGFB</i> fusion	<i>COL1A1</i> breakpoint: 5' <i>COL1A1</i> gain	Split <i>COL1A1</i> : +	
13	43/F	Thigh	Dermatofibrosarcoma protuberans	<i>COL1A1-PDGFB</i> fusion	<i>COL1A1</i> breakpoint: 5' <i>COL1A1</i> gain	Split <i>COL1A1</i> : +	
14	40/M	Forehead	Dermatofibrosarcoma protuberans	<i>COL1A1-PDGFB</i> fusion	<i>COL1A1</i> breakpoint: 5' <i>COL1A1</i> gain	Split <i>COL1A1</i> : +	
15	37/F	Cheek	Dermatofibrosarcoma protuberans	<i>COL1A1-PDGFB</i> fusion	<i>COL1A1</i> breakpoint: 5' <i>COL1A1</i> gain	Split <i>COL1A1</i> : +	
16	38/M	Neck	Dermatofibrosarcoma protuberans	<i>COL1A1-PDGFB</i> fusion	ND	Split <i>COL1A1</i> : +	

17	73/F	Arm	Dermatofibrosarcoma protuberans	<i>COL1A1-PDGFB</i> fusion	ND	Split <i>COL1A1</i> : +	
18	29/F	Shoulder	Fibrosarcoma	<i>COL1A1-PDGFB</i> fusion	ND	Split <i>COL1A1</i> : -	
19	29/F	Breast	Dermatofibrosarcoma protuberans	<i>COL6A3-PDGFD</i> fusion (frozen)	<i>COL6A3</i> breakpoint: 5' <i>COL6A3</i> gain	Split <i>PDGFD</i> : + Split <i>COL6A3</i> : +	<i>COL6A3-PDGFD</i> fusion
20	4/M	Calf	Pigmented dermatofibrosarcoma protuberans	No fusion transcript	No breakpoint	Split <i>PDGFD</i> : - Split <i>COL6A3</i> : - Split <i>EMILIN2</i> : -	

Table 1. Clinical and molecular features of the cohort of dermatofibrosarcoma protuberans variants.

Abbreviations: M, male; F, female; RNA sequencing, ribonucleic acid sequencing; FISH, fluorescence in situ hybridization; ND, not done.

Figure 1

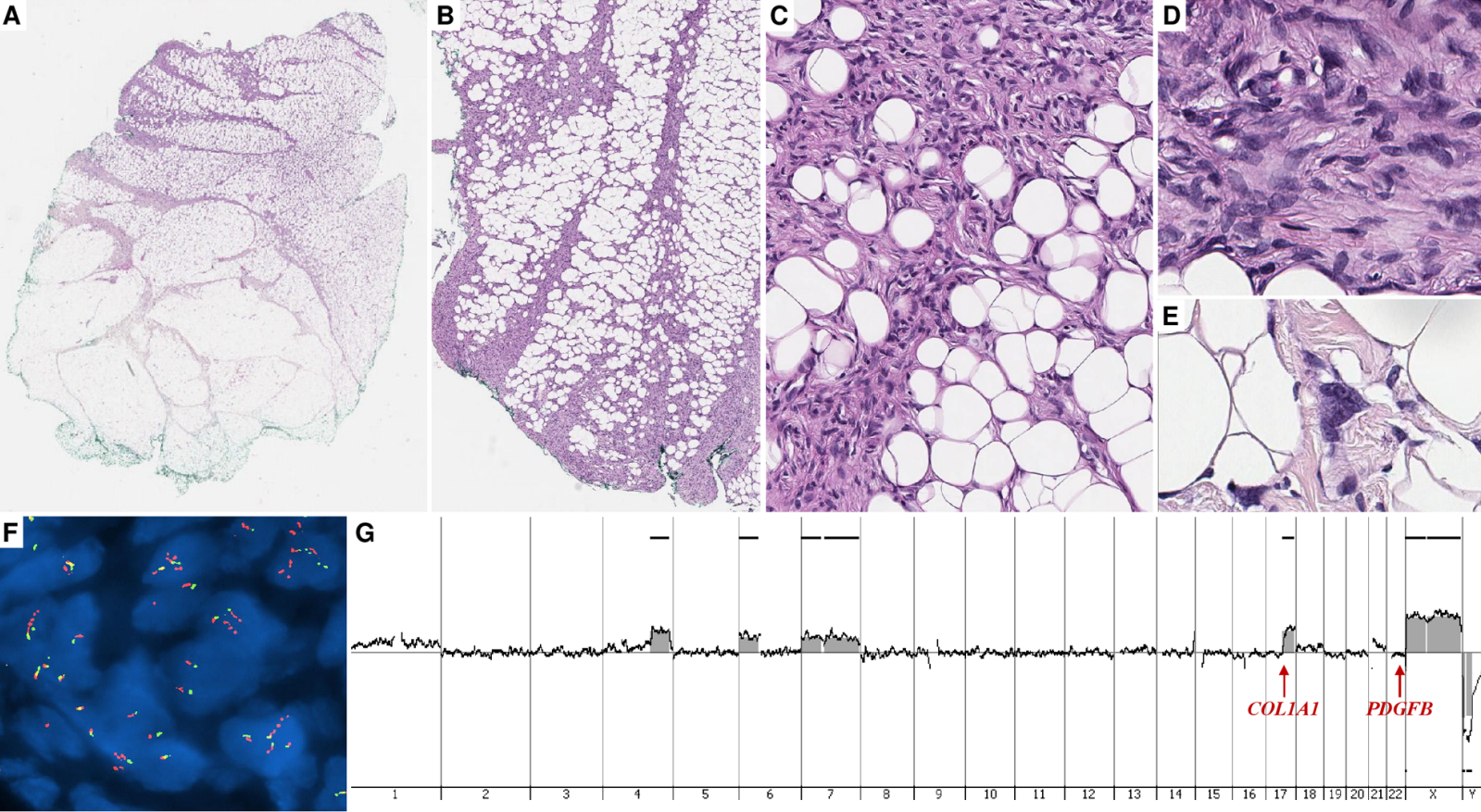


Figure 2

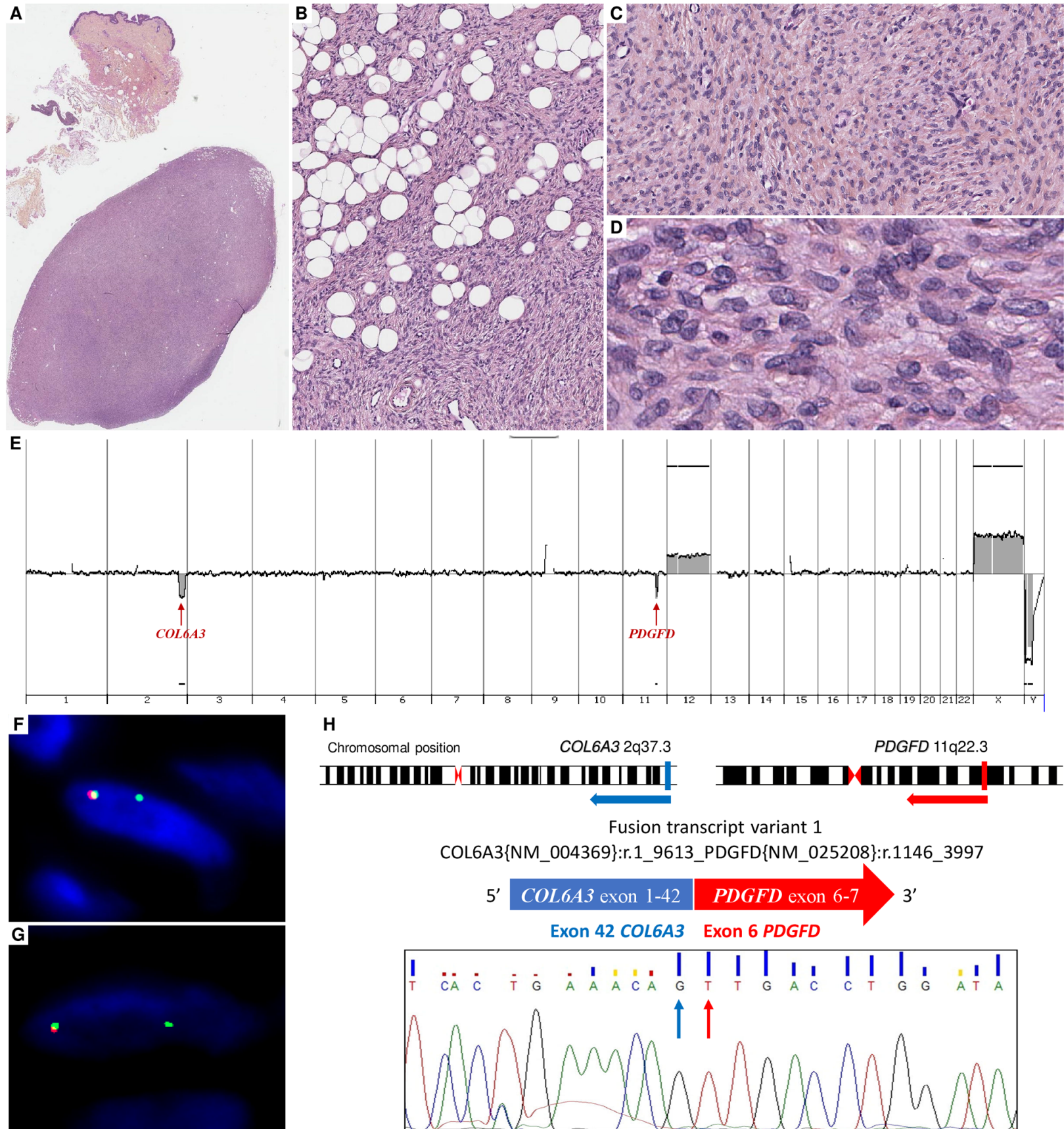


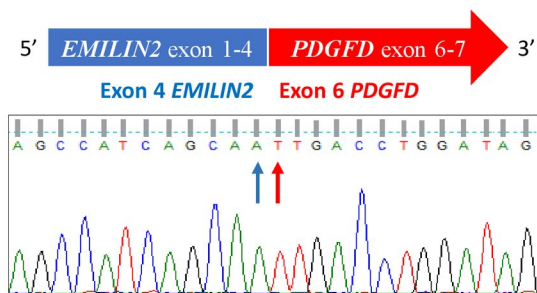
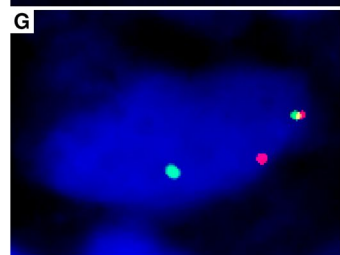
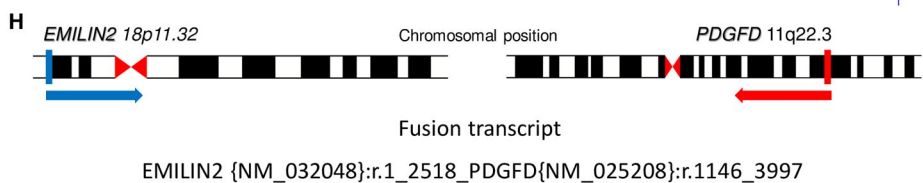
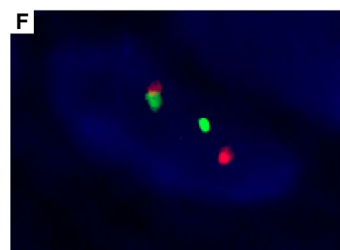
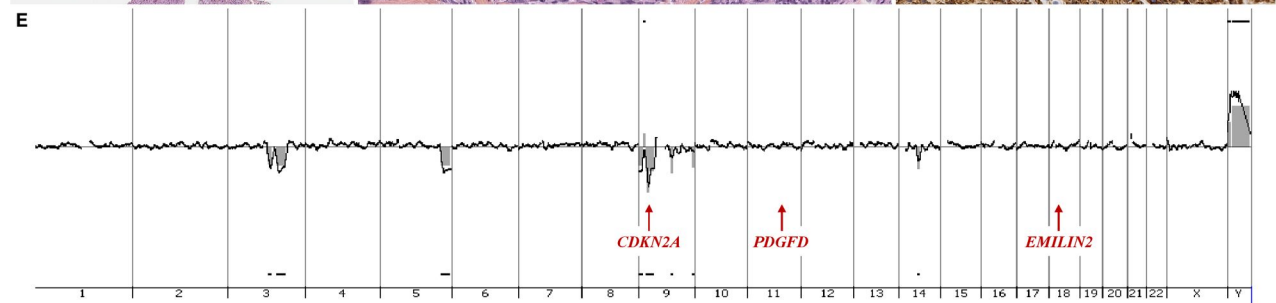
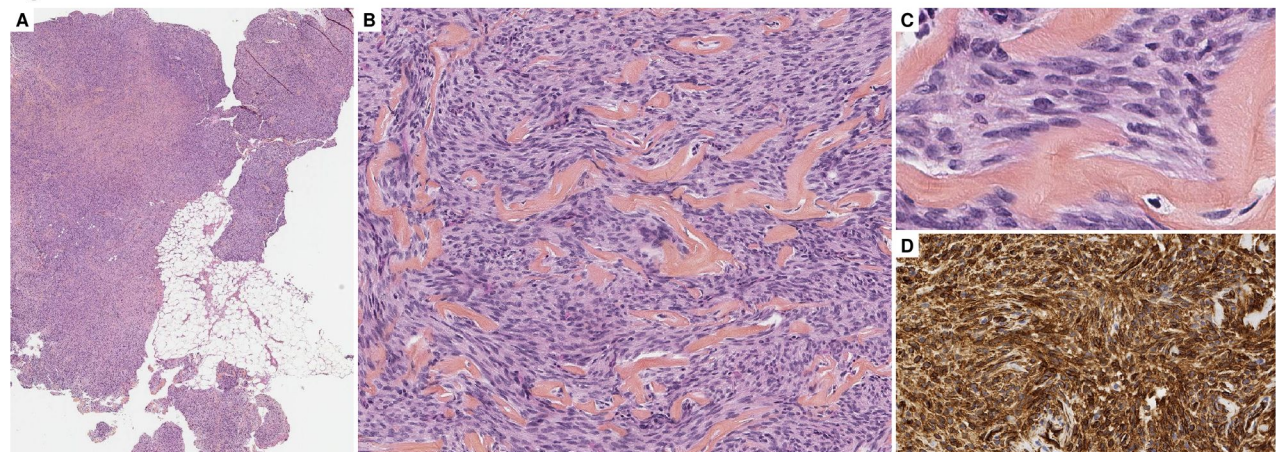
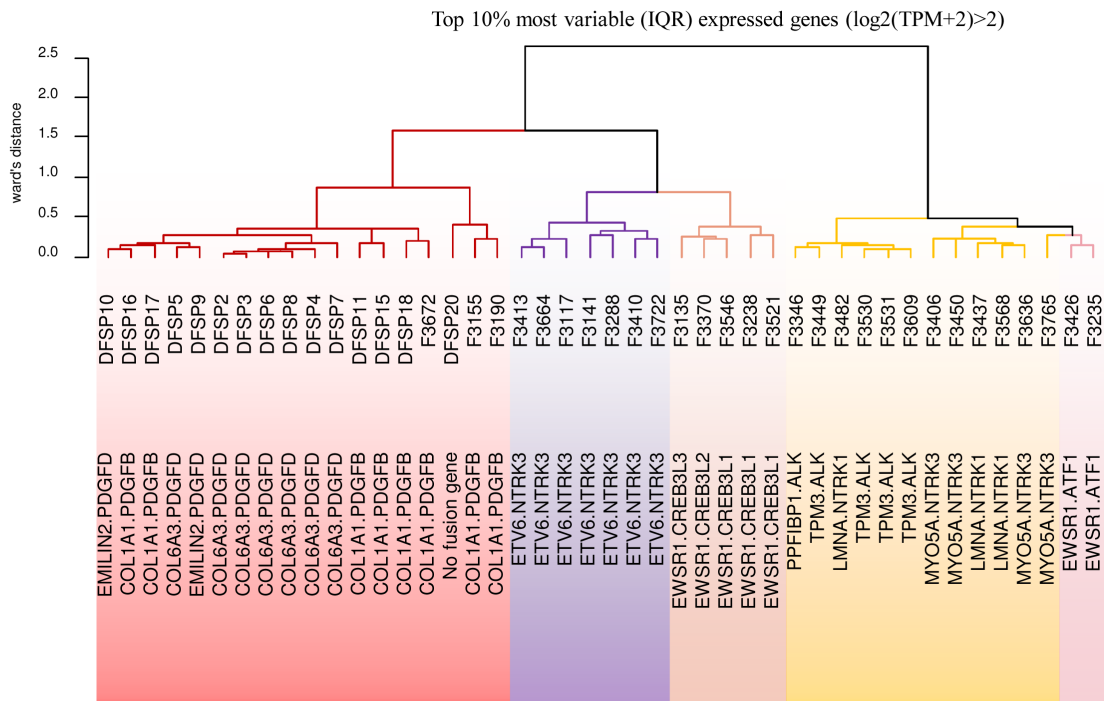
Figure 3

Figure 4



Case #	Diagnosis	Location	Tumor site	Architecture	Additional feature	CD34 staining	Mitotic index (/10HPF)	Infiltration pattern	Clinical presentation	Relapse	Follow-up (months after surgery)
1	Dermatofibrosarcoma protuberans	abdominal wall	hypodermis	storiform	-	diffuse +	0	honeycomb	-	no	25
2	Dermatofibrosarcoma protuberans	breast	hypodermis	storiform	focal hemangiopericytic vessels, S100 focally +, no pigment	diffuse +	1	honeycomb	-	no	12
3	Dermatofibrosarcoma protuberans	chest wall	dermo-hypodermis	storiform	focal hemangiopericytic vessels	diffuse +	1	honeycomb	pseudo scar	at 11 years	37 since relapse 1
4	Dermatofibrosarcoma protuberans	chest wall	dermo-hypodermis	storiform	-	diffuse +	1	honeycomb	-	no	55
5	Dermatofibrosarcoma protuberans	shoulder	dermo-hypodermis	storiform	fibrous	diffuse +	0	honeycomb	-	NA	NA
6	Dermatofibrosarcoma protuberans	back	dermis	storiform	focally fibrous	diffuse +	0	honeycomb	nodule	no	15
7	Dermatofibrosarcoma protuberans	breast	dermo-hypodermis	storiform	-	diffuse +	1	honeycomb	nodule with red discoloration	no	10
8	Dermatofibrosarcoma protuberans	chest wall	dermo-hypodermis	storiform	-	diffuse +	0	honeycomb	-	no	69
9	Fibrosarcoma	leg	hypodermis	fascicles	fibrous	heterogeneous +	5	well delineated	-	delayed resection at 6 months	4

10	Fibrosarcoma	leg	hypodermis	fascicles	focally pigmented and fibrous, S100 -	diffuse +	4	well delineated	-	no	10
11	Dermatofibrosarcoma protuberans	back	dermo-hypodermis	storiform	fibrous	diffuse +	2	honeycomb	-	unresectable	NA
12	Fibrosarcoma	thigh	dermo-hypodermis	fascicles	-	diffuse +	6	honeycomb	-	no	47
13	Dermatofibrosarcoma protuberans	thigh	dermo-hypodermis	storiform	fibrous	diffuse +	1	honeycomb	multinodular (2 juxtaposed nodules)	no	51
14	Dermatofibrosarcoma protuberans	forehead	dermo-hypodermis	storiform	-	diffuse +	0	honeycomb	-	no	51
15	Dermatofibrosarcoma protuberans	cheek	dermo-hypodermis	storiform	focal giant cell	diffuse +	0	honeycomb	pseudo scar	no	68
16	Dermatofibrosarcoma protuberans	neck	dermo-hypodermis	storiform	-	diffuse +	1	honeycomb	-	no	8
17	Dermatofibrosarcoma protuberans	arm	dermo-hypodermis	storiform	-	diffuse +	0	honeycomb	slow growing pseudo-plaque	2 relapses at 10 and 12 years	57 since relapse 2
18	Fibrosarcoma	shoulder	dermo-hypodermis	fascicles	-	diffuse +	20	honeycomb	-	no	6
19	Dermatofibrosarcoma protuberans	breast	hypodermis	storiform	-	diffuse +	1	honeycomb	-	no	24
20	Bednar tumor	calf	dermo-hypodermis	storiform	focally S100 +, no pigment	diffuse +	0	honeycomb	vascular-like red plaque	no	17

Supplementary Table 1

Supplementary Table 2.

FISH design	BAC	Cytoband	Gene	Labelling
<i>PDGFD</i> break-apart	CTD-2531F7	11q22.3	<i>5'PDGFD</i>	red signal
<i>PDGFD</i> break-apart	RP11-746G21	11q22.3	<i>3'PDGFD</i>	green signal
<i>COL6A3</i> break-apart	CTD-3149I15	2q37.3	<i>3'COL6A3</i>	red signal
<i>COL6A3</i> break-apart	CTD-3082D1	2q37.3	<i>5'COL6A3</i>	green signal
<i>EMILIN2</i> break-apart	RP11-92C22	18p11.32	<i>5'EMILIN2</i>	green signal
<i>EMILIN2</i> break-apart	CTD-2379D18	18p11.32	<i>3'EMILIN2</i>	red signal

Case #	Fusion transcript	FISH COL1A1-PDGFB fusion	FISH PDGFB break apart	FISH COL1A1 break apart	FISH PDGFD break apart	FISH COL6A3 break apart	FISH EMILIN2 break apart	Intragenic breakpoint by array-comparative genomic hybridization	Additional quantitative anomalies
1	<i>COL6A3(e42)-PDGFD</i> (e6)	Negative	Negative	NA	Split	Split	NA	Loss of 3' <i>COL6A3</i> region (2q37.3)	No
2	<i>COL6A3(e42)-PDGFD</i> (e6)	ND	Negative	NA	Split	Split	NA	<i>PDGFD</i> intragenic deletion	Loss of 11q22.3
3	<i>COL6A3(e43)-PDGFD</i> (e6)	Negative	Negative	Negative	Split	Split	NA	<i>PDGFD</i> intragenic deletion	Loss of 11q22.4
4	<i>COL6A3(e42)-PDGFD</i> (e6)	Negative	Negative	Negative	Failure	Failure	NA	<i>PDGFD</i> intragenic deletion	Losses of 11q22.5 and 2q33-q37
5	<i>COL6A3(e42)-PDGFD</i> (e6)	ND	Negative	Negative	ND	ND	NA	Losses of 5' <i>PDGFD</i> and 3' <i>COL6A3</i>	Losses of 3q26, 2q37, 11q22
6	<i>COL6A3(e42)-PDGFD</i> (e6)	ND	Negative	Negative	Split	Split	NA	Losses of 5' <i>PDGFD</i> and 3' <i>COL6A3</i>	Gain of whole chromosome 12; Losses of 2q35-q37 and 11q22
7	<i>COL6A3(e42)-PDGFD</i> (e6)	Failure	Negative	Negative	Split	Split	NA	Failure	Failure
8	<i>COL6A3(e42)-PDGFD</i> (e6)	Negative	NA	NA	Split	Failure	NA	ND	ND
9	<i>EMILIN2(e4)-PDGFD</i> (e6)	Negative	Negative	NA	Split	NA	Split	No breakpoint	Losses of 3q, 5q, 9p, 9q and 14q, homozygous deletion of <i>CDKN2A</i>
10	<i>EMILIN2(e4)-PDGFD</i> (e6)	Negative	Negative	NA	Split	NA	Split	<i>PDGFD</i> intragenic deletion	Homozygous deletion of <i>CDKN2A</i>

11	COL1A1(e45)- PDGFB(e2)	Negative	Negative	Split	NA	NA	NA	5'COL1A1 gain	Gains of 1q21-q25.3, 17q21.33-qter whole chromosomes 6 and 10 and loss of 1q22-23.1
12	COL1A1(e33)- PDGFB(e2)	Negative	Negative	Split	NA	NA	NA	5'COL1A1 gain	Losses of 6q12-q26 and of 8p and gains of 17q21-qter and of 22q11- q12 region
13	COL1A1(e11)- PDGFB(e2)	Negative	Negative	Split	NA	NA	NA	5'COL1A1 gain	Gains of 1p33-q23, 2q37-qter, 16p13-p12 and 17q21-qter
14	COL1A1(e46)- PDGFB(e2)	Negative	Negative	Split	NA	NA	NA	5'COL1A1 gain	Gains of 7pter-q11 region and 17q21-qter
15	COL1A1(e20)- PDGFB(e2)	Negative	Negative	Split	NA	NA	NA	5'COL1A1 gain	Gains of 4q28-q35, 6p, chr7 and 17q21-qter
16	COL1A1(e43)- PDGFB(e2)	ND	Negative	Split	NA	NA	NA	ND	ND
17	COL1A1(e39)- PDGFB(e2)	Ambiguous	Negative	Split	NA	NA	NA	ND	ND
18	COL1A1(e40)- PDGFB(e2)	Negative	Negative	Negative, polysomy	NA	NA	NA	ND	ND
19	COL6A3(e42)- PDGFD (e6)	Negative	NA	NA	Split	Split	NA	5'COL6A3 gain	Gains of 1, 2q, 7, 17,11q (spanning PDGFD)
20	No fusion transcript	ND	Negative	Negative	Negative	Negative	Negative	No breakpoint	Loss of 2p26-p22

Supplementary Table 3.

Supplementary Table 4.

Sample ID	Histotype	Fusion gene
F3672	« conventional » dermatofibrosarcoma protuberans	<i>COL1A1-PDGFB</i>
F3155	« conventional » dermatofibrosarcoma protuberans	<i>COL1A1-PDGFB</i>
F3190	« conventional » dermatofibrosarcoma protuberans	<i>COL1A1-PDGFB</i>
F3413	infantile fibrosarcoma	<i>ETV6-NTRK3</i>
F3664	infantile fibrosarcoma	<i>ETV6-NTRK3</i>
F3117	infantile fibrosarcoma	<i>ETV6-NTRK3</i>
F3141	infantile fibrosarcoma	<i>ETV6-NTRK3</i>
F3288	infantile fibrosarcoma	<i>ETV6-NTRK3</i>
F3410	infantile fibrosarcoma	<i>ETV6-NTRK3</i>
F3722	infantile fibrosarcoma	<i>ETV6-NTRK3</i>
F3135	low grade fibromyxoid sarcoma	<i>EWSR1-CREB3L3</i>
F3370	low grade fibromyxoid sarcoma	<i>EWSR1-CREB3L2</i>
F3546	low grade fibromyxoid sarcoma	<i>EWSR1-CREB3L1</i>
F3238	low grade fibromyxoid sarcoma	<i>EWSR1-CREB3L1</i>
F3521	low grade fibromyxoid sarcoma	<i>EWSR1-CREB3L1</i>
F3426	clear cell sarcoma of soft tissue	<i>EWSR1-ATF1</i>
F3235	clear cell sarcoma of soft tissue	<i>EWSR1-ATF1</i>
F3346	Spitzoid neoplasm	<i>PPFIBP1-ALK</i>
F3449	Spitzoid neoplasm	<i>TPM3-ALK</i>
F3482	Spitzoid neoplasm	<i>LMNA-NTRK1</i>
F3530	Spitzoid neoplasm	<i>TPM3-ALK</i>
F3531	Spitzoid neoplasm	<i>TPM3-ALK</i>
F3609	Spitzoid neoplasm	<i>TPM3-ALK</i>
F3406	Spitzoid neoplasm	<i>MYO5A-NTRK3</i>
F3450	Spitzoid neoplasm	<i>MYO5A-NTRK3</i>
F3437	Spitzoid neoplasm	<i>LMNA-NTRK1</i>
F3568	Spitzoid neoplasm	<i>LMNA-NTRK1</i>
F3636	Spitzoid neoplasm	<i>MYO5A-NTRK3</i>
F3765	Spitzoid neoplasm	<i>MYO5A-NTRK3</i>